Research Square

Preprints are preliminary reports that have not undergone peer review.
They should not be considered conclusive, used to inform clinical practice,
or referenced by the media as validated information.

Longitudinal deterioration and rainfall-associated variation in the water quality of the Gosthani River, a small regulated river on the east coast of India: 13 monthly campaigns at ten stations

B. Vijaya Saradhi

Andhra University College of Engineering (A), Andhra University

Mohammad Mdhour ahmad abuqrian

mohammedmadhour@gmail.com

Andhra University College of Engineering (A), Andhra University

Research Article

Keywords: Faecal indicator bacteria, Ammonia, Estuarine mixing, Monitoring network design, Repeated-measures design, Bay of Bengal

Posted Date: October 30th, 2026

DOI: https://doi.org/10.21203/rs.3.rs-11322457/v1

License: This work is licensed under a Creative Commons Attribution 4.0 International License. Read Full License

Additional Declarations: No competing interests reported.

Abstract

Small rivers carry land-based pollution to tropical coasts but are seldom monitored, so the reaches where deterioration begins are rarely known. We sampled ten main-stem stations of the Gosthani River, east coast of India, in 13 monthly campaigns (September 2025–September 2026) to locate deterioration hotspots and to identify what a fixed-station design can and cannot resolve. Water quality changed little above the Thatipudi reservoir but deteriorated steeply in the 30 km below it. Median biochemical oxygen demand (BOD) rose from 1.70 mg/L below the dam to 12.25 mg/L at the lowest riverine station. The geometric mean of *Escherichia coli* rose from 465 to 3,136 most probable number (MPN)/100 mL, and median dissolved-oxygen saturation fell to 63%. The largest increments were concentrated in two reaches containing towns and villages. In a screening comparison, BOD exceeded the national Class C value of 3 mg/L in every usable campaign at the four lowest stations, where ammonia-N formed 57–76% of inorganic nitrogen. Within stations, antecedent rainfall was associated with higher suspended solids and lower conductivity; with only 12–13 shared campaigns, these associations are exploratory. At the estuary, seawater formed less than 2% of the water, yet BOD and total phosphorus were 44–46% lower than upstream. Interpreting this contrast requires measurements of lateral inflow. The spatial pattern is consistent with wastewater-associated loading, but sources were not apportioned and discharge was not measured. Four stations captured the gradient. This supports a compact monitoring design that pairs these stations with discharge gauging and rainfall-timed sampling.

Introduction

Rivers are major pathways by which land-based pollution reaches the coastal ocean, and in monsoonal Asia much of that pathway runs through small rivers that drain directly to the sea. First-order and other small streams make up most of the length of the world’s river networks (Downing et al., 2012; Wohl, 2017), and headwater streams supply a large share of the water and nitrogen carried by downstream rivers (Alexander et al., 2007). Yet monitoring networks are disproportionately concentrated on large, perennial rivers (Krabbenhoft et al., 2022), and the number of gauges contributing to global datasets has declined (Ruhi et al., 2018). In the 2023 reporting round for Sustainable Development Goal indicator 6.3.2, only about 3% of the data used came from the poorer half of United Nations member states (UNEP, 2024). Small rivers that carry sewage, sediment and nutrients from towns to the coast therefore remain poorly described.

The east coast of India illustrates this gap. The estuaries of large monsoonal rivers have been studied in detail. In the Godavari, nutrient loading is dominated by monsoon discharge and phytoplankton biomass is limited by suspended sediment (Sarma et al., 2010). Reduced discharge there lengthened flushing time and intensified blooms (Acharyya et al., 2012), and nitrate isotopes identified nitrified soil and sewage nitrogen as important sources (Sridevi et al., 2023). In the Mahanadi, discharge and tides control salinity, whereas point sources influence phosphate and ammonium (Acharyya et al., 2021; Pattanayak et al., 2024). At the scale of the Indian peninsula, much of the dissolved inorganic nitrogen carried by monsoonal rivers is retained or removed before it reaches the coast (Krishna et al., 2016). Small rivers with lagoonal estuaries and regulated flow are comparatively poorly represented in this literature.

The coast of Visakhapatnam, the largest city of Andhra Pradesh, shows why this gap matters. Beach water and sediment at seven land-drainage outfalls were hygienically poor, and one beach was unsuitable even for non-contact recreation (Clark et al., 2003). Faecal indicator and pathogenic bacteria in the coastal Bay of Bengal off the city remained above standard limits throughout the year (Sudha Rani et al., 2018). The rivers draining this coast have received much less attention. The Nagavali and Vamsadhara rivers, for example, were sampled before and after one monsoon in recent multivariate studies, without measurements of faecal indicators (Saikrishna et al., 2024a, b). In India, a river stretch is included in the national polluted-stretch inventory on the basis of monitoring information (CPCB, 2022), so small rivers without routine monitoring can remain under-represented.

The Gosthani River is one such river. It rises in the karst of the Borra Caves in the Eastern Ghats and supplies drinking water to Visakhapatnam from the Thatipudi reservoir. It then crosses an agricultural plain with small towns and reaches the Bay of Bengal through a tidal lagoon at Bheemunipatnam, where a bivalve fishery operates (Rama Rao et al., 2024). The literature reviewed for this study did not identify a full-year water-quality record for the river, and the CPCB list of water-quality stations on medium and minor rivers for 2023 contains no station on its main stem. The two stations listed as “Gostani” in that list are at Vendra, Palakoderu mandal, on a different watercourse of the same name in the Godavari delta (CPCB, 2023). We therefore sampled ten stations from the headwater to the estuary in 13 monthly campaigns and addressed four questions:

1. How does water quality change from the forested headwater to the estuary, and where is the strongest deterioration located?
2. Is campaign-to-campaign variation within stations associated with antecedent rainfall, as distinct from calendar season?
3. How do concentrations change between the last riverine station and the estuary, relative to what seawater mixing alone would produce?
4. What do the observations imply for monitoring the river and protecting the receiving coastal waters?

The study is observational. Discharge was not measured, pollution sources were not apportioned, and the interpretation of mechanisms is accordingly limited.

Materials and methods

Study area

The Gosthani basin lies between approximately 17.9° and 18.3° N and 82.9° and 83.5° E (Fig. 1). The monitored main stem falls from 740 m at the headwater station (S01) to 2.6 m at the estuary (S10) over a chord distance of 69.6 km, with about three-quarters of the elevation loss occurring between S01 and S02. The upper basin comprises khondalite, charnockite and granitic gneiss of the Eastern Ghats, with a carbonate body at the Borra Caves (Sriramadas & Murty, 1975; Le Bas et al., 2002), and is deeply weathered to lateritic soils. The Thatipudi reservoir supplies drinking water to Visakhapatnam. It divides the river into a forested upper basin and an agricultural lower basin containing the towns of Srungavarapukota, Lakkavarapukota and Jami. Rainfall occurs mainly during the south-west (June–September) and north-east

(October–November) monsoons. Over the study year, the mean of the two satellite products used here gave approximately 1,628 mm over the S01 catchment and 897 mm over the S10 catchment. The estuary is a shallow lagoon of approximately 120 ha behind a sand spit (Shivani & Rao, 1996; Ganesh et al., 2013) and is used for bathing and bivalve harvesting (Rama Rao et al., 2024).

Sampling design

Ten stations were established on the main stem from Katiki waterfall (S01) to the estuary at Bheemunipatnam (S10) (Table 1). All ten stations were sampled in 13 campaigns at approximately monthly intervals: 18 September 2025, 16 October 2025, 20 November 2025, 15 December 2025, 23 January 2026, 19 February 2026, 17 March 2026, 19 April 2026, 21 May 2026, 20 June 2026, 14 July 2026, 9 August 2026 and 13 September 2026. Campaign dates were taken from the signed laboratory reports and used consistently in the rainfall linkage and in all campaign-based analyses. Because the series begins and ends in September and the July 2026 laboratory results were excluded (below), the 12 campaigns with laboratory data contain two September samples and no July sample. Station summaries therefore describe the sampled campaigns, not a calendar-balanced annual mean. For descriptive comparisons, campaigns were grouped into the dry season (December–May; six campaigns), the north-east monsoon (October–November; two campaigns) and the south-west monsoon (June–September; five campaigns, four with laboratory data). Calendar season was not used as an explanatory variable, because antecedent rainfall described conditions at sampling more directly (see Results).

Table 1
Sampling stations: setting, elevation, chord distance from S01, delineated catchment area and selected land-cover classes (Dynamic World, January–March 2026). Other classes (e.g. shrub and scrub, grass, bare ground and water) make up the remainder.

Station	Setting	Elev. (m)	Distance (km)	Catchment (km²)	Trees (%)	Crops (%)	Built (%)
S01	Katiki waterfall	740	0.0	50.0	57.0	3.5	1.2
S02	Below Borra Caves	186	9.4	130.5	69.7	2.7	0.8
S03	Road toll gate	106	17.2	225.0	77.4	2.1	0.8
S04	Gosthani bridge	94	20.8	238.5	77.6	2.0	0.8
S05	Above reservoir	91	21.7	243.0	77.7	2.0	0.8
S06	Below dam outfall	67	27.3	321.3	76.6	1.7	0.7
S07	Jami bridge	29	41.5	745.2	66.8	12.7	2.7
S08	Bhimasingi bridge	23	46.8	1,101.9	63.1	16.6	3.7
S09	Pandrangi bridge	9	57.6	1,319.6	62.7	17.5	4.0
S10	Estuary, Bheemunipatnam	3	69.6	1,558.5	59.4	19.9	5.3

Elevation from Copernicus GLO-30; catchments by D8 flow routing.

At each station and campaign, a single grab sample was collected, and temperature, pH and dissolved oxygen were measured once in the field. All ten stations were sampled on each campaign date. The design yields 130 station-campaign observations. These are repeated measurements at ten fixed, hydrologically nested stations under 13 shared sampling conditions, not 130 independent replicates. Field observations of activities at and near the stations (domestic use of the river, visitor use, road traffic and sewage entering the river) were noted during the campaigns as qualitative context. They were not recorded systematically by reach and were not used in any statistical analysis.

Laboratory analysis and quality assurance

Temperature and dissolved oxygen (DO) were measured in the field with a Lutron DO-5509 meter, and pH with a Hanna pHep meter. The other 21 determinands were analysed by a commercial environmental laboratory accredited to ISO/IEC 17025:2017 (NABL certificate TC-15009, valid 2 December 2024 to 1 December 2028, i.e. throughout the study period). These were turbidity, electrical conductivity (EC), total dissolved and suspended solids (TDS and TSS), chemical oxygen demand (COD), biochemical oxygen demand (BOD), nitrate, ammonia-N, total phosphorus (TP), sulphate, fluoride, iron, sodium, potassium, total hardness, total alkalinity, chloride, arsenic, cadmium, lead and *Escherichia coli*. Analyses followed Standard Methods, 24th edition (APHA et al., 2023), and IS 3025 (Part 44) for BOD (BIS, 1993). The methods printed on the laboratory reports were (Standard Methods section numbers): turbidity 2130 B; EC 2510 B; TDS 2540 C; TSS 2540 D; COD 5220 D; nitrate and sulphate 4110 B (ion chromatography); ammonia-N 4500-NH_3 B and F; total phosphorus 4500-P B and E; fluoride 4500-F^- C; chloride 4500-Cl^- B; sodium 3500-Na B; potassium 3500-K B; total hardness 2340 C; total alkalinity 2320 B; iron 3030 E with 3500-Fe B (total iron after nitric-acid digestion); arsenic, cadmium and lead 3125 (ICP-MS); and *E. coli* 9223 B. BOD was measured over 3 days at 27°C, the Indian standard condition. IS 3025 (Part 44) adopts this condition to give values comparable to the conventional 5-day, 20°C test, but no study-specific conversion was available, so comparisons with 5-day BOD values should be read as approximate. Nitrate is reported as nitrate (NO_3^-); for dissolved inorganic nitrogen (DIN), it was converted to nitrate-N (NO_3-N = 0.226 × NO_3^-). *Escherichia coli* was enumerated as the most probable number (MPN) per 100 mL by the enzyme-substrate method (APHA 9223 B). Twenty-six samples from S08–S10 were diluted 1:10 before enumeration, and no result was reported as exceeding the upper counting limit.

The reporting limit was 0.0005 mg/L for Cd and Pb. Values below the reporting limit were treated as censored and were not replaced by zero or by a fraction of the limit. Censored values were excluded from summary statistics and from rank-based tests (complete-case analysis); for lead, this reduced the Friedman test to the five campaigns in which lead was detected at every station. Of the 2,730 laboratory values (21 determinands × 130 observations), 170 were excluded. These were the results for 17 determinands from 14 July 2026, which a university laboratory analysed and whose recorded locations did not correspond to the sampling stations. For that campaign, only iron and the three trace metals, analysed by the commercial laboratory, were retained.

Field calibration records were available for all 13 campaigns. For the DO/temperature meter, zero-oxygen checks were 0.00–0.02 mg/L and air-saturation checks were 99.0–100.1%. The pH buffer checks were

7.00–7.02 (pH 7 buffer) and 4.00–4.02 (pH 4 buffer), and reference-thermometer checks differed from the field thermometer by 0.0–0.1°C. All recorded checks were marked as accepted. The laboratory's accreditation covers its procedures but does not by itself establish the accuracy of individual results. Method-specific QA/QC data for these sample batches (blanks, duplicates, spike recoveries and measurement uncertainty) were not available to the authors and have not been inferred. The analytical precision and bias of individual results are therefore unknown, and differences close to a criterion value should be interpreted with caution.

Catchment delineation, land cover and rainfall

The catchment of each station was delineated from the Copernicus GLO-30 digital elevation model (European Space Agency, n.d.) using D8 flow routing, with each station snapped to the cell of maximum flow accumulation within 150 m. The delineated catchment at the Thatipudi dam (321.3 km², at S06) was within 3.4% of the official figure (332.72 km²; Water Resources Department, Government of Andhra Pradesh, n.d.), and the catchment at S10 was within 1.8% of the HydroSHEDS basin (Lehner & Grill, 2013). Land cover was derived from Dynamic World (Brown et al., 2022), which classifies Sentinel-2 imagery at 10 m (Drusch et al., 2012), using the most frequent class at each pixel between January and March 2026. Daily rainfall over each catchment was calculated as the mean of CHIRPS (Funk et al., 2015) and IMERG V07 (Huffman et al., 2023). Each observation was characterised by the catchment rainfall accumulated over the preceding 7 and 30 days, ending on the campaign date.

Indicative river discharge

No gauge operates on the monitored reach and discharge was not measured. To place campaigns in broad hydrological classes, daily discharge was taken from the GloFAS-ERA5 reanalysis, version 4.0 (Harrigan et al., 2020; Copernicus Emergency Management Service, n.d.; 0.05° grid), at the cell on the channel network adjacent to each station. The only gauge in the basin, at Kasipatnam, lies 0.6 km from S03 and has daily records for 2001–2011 (3,362 days used; AP State Water, n.d.). The modelled series at the S03 cell was bias-corrected by empirical quantile mapping (Gudmundsson et al., 2012), fitted on 2001–2007 and tested on 2008–2011 (953 days). Performance was evaluated with the Kling–Gupta efficiency (KGE; Gupta et al., 2009), the Nash–Sutcliffe efficiency (NSE; Nash & Sutcliffe, 1970) and percentage bias at daily and monthly resolution. Skill was not evaluated for 7-day means, the averaging period used for campaign values, so the accuracy of the campaign values is unknown. Uncertainty in the correction was represented by 200 year-block bootstrap resamples (P10–P90). This represents uncertainty in the correction parameters only, not the structural error of the model.

Discharge at S04 and S05, which lie above the reservoir, was obtained by scaling the S03 estimate by catchment area (ratios 1.06 and 1.08). Discharge below the Thatipudi dam (S06–S10) depends on unrecorded releases. It was bracketed by three assumed scenarios, each added to the GloFAS flow from the area between the dam and the station:

- Scenario A: no release.

- Scenario B: release of the corrected inflow minus the reported drinking-water supply of 0.58 $m^3 s^{-1}$ (11 million imperial gallons per day; Water Resources Department, Government of Andhra Pradesh, n.d.), during August–November only.
- Scenario C: the GloFAS dam-cell outflow.

S01 and S02 were not estimated because no calibration site exists upstream of S03. Campaign values are 7-day means ending on the sampling date. All estimates are given in Online Resource 1. Modelled discharge was used only for classification and for exploratory, supplementary correlations. It was not used to calculate loads.

Data analysis

The analyses were organised in two tiers: primary analyses of the spatial pattern and exploratory analyses of temporal and multivariate structure.

Primary analyses (spatial pattern). Station differences were tested with the Friedman test (Friedman, 1937). Campaign was the block and station the treatment, using the campaigns with complete station-by-campaign data for each determinand (12 for laboratory determinands, 13 for field determinands, iron and trace metals). The Friedman test asks whether stations are ranked consistently across campaigns. It does not assume independence between stations within a campaign, which is appropriate for nested stations sampled on the same day. The strength of the station effect can be expressed as Kendall's coefficient of concordance, $W = \chi^2 / [n\,(k-1)]$, where n is the number of campaigns (blocks) and $k = 10$ stations; values for every determinand are given in Online Resource 2. Pairwise station comparisons were not used for inference. With 12 paired campaigns, the smallest attainable two-sided p value of an exact Wilcoxon signed-rank test is 0.00049. Holm adjustment (Holm, 1979) across the 45 station pairs would therefore detect only pairs in which one station exceeded the other in 11 or 12 of 12 campaigns. Reach-to-reach changes are instead described by the differences in station medians (Table 3).

Exploratory analyses (temporal variation, multivariate structure, discharge, catchment attributes). No p value from these analyses is interpreted as confirmatory.

- *Rainfall association.* Each determinand was ranked within station to remove the downstream gradient, and the ranks were correlated with 7- and 30-day catchment rainfall using Spearman's ρ (Spearman, 1904). The pooled coefficient is reported as a descriptive measure of association. Its nominal p value treats 120 observations as independent, whereas all stations share the same 12–13 sampling conditions, so nominal p values are not reported and no formal significance test of the rainfall associations is claimed.
- *Multivariate structure.* Principal component analysis (PCA) was applied to 20 determinands (temperature, pH, DO, turbidity, EC, TDS, TSS, COD, BOD, nitrate, ammonia-N, TP, sulphate, iron, sodium, potassium, total hardness, total alkalinity, chloride and *E. coli*). These are the variables shown in Fig. 5a. It used the 120 observations from the 12 campaigns with complete laboratory data. Cadmium (all values censored) and lead (28 censored values) were not included, nor were fluoride and arsenic.

Skewed variables were $\log_{10}$-transformed, all variables were standardised, and components with eigenvalues > 1 were retained and varimax-rotated (Kaiser, 1958). The Kaiser–Meyer–Olkin measure and Bartlett's test (Bartlett, 1950; Kaiser, 1970) are reported descriptively. Both assume independent observations and overstate the evidence when applied to repeated measures. Stations were grouped by hierarchical clustering of standardised station medians using Ward's method (Ward, 1963).

- *Modelled discharge.* Estimated discharge was related to each determinand by Spearman correlation within each of stations S03–S10 (n = 12 campaigns for laboratory determinands; 13 for field determinands and metals).
- *Catchment attributes.* Station medians were related to catchment attributes (n = 10 nested catchments; critical $|\rho| = 0.648$ at $\alpha = 0.05$). Because the catchments are nested, these coefficients describe co-variation along the river and are not tests of land-use effects.

DO saturation was calculated from field temperature using Standard Methods (APHA et al., 2023), with elevation correction. The un-ionised fraction of ammonia was calculated from temperature and pH (Emerson et al., 1975). Analyses and figures were produced in Python with pandas, NumPy, SciPy (Friedman and Spearman tests, linear regression, Ward clustering) and Matplotlib; the PCA, varimax rotation, Kaiser–Meyer–Olkin measure and Bartlett's test were implemented directly in NumPy. The analysis was re-executed for this paper in Python 3.13 with NumPy 2.5.3, pandas 3.0.5, SciPy 1.18.1 and Matplotlib 3.11.2. Land-cover statistics for each catchment were computed in Google Earth Engine.

Estuarine mixing. The seawater fraction at S10 in each campaign was estimated from chloride with a two-end-member model between S09 (river) and standard seawater:

$$f = \frac{\mathrm{Cl}_{10} - \mathrm{Cl}_{09}}{\mathrm{Cl}_{sw} - \mathrm{Cl}_{09}} \quad (1)$$

where Cl_{10} and Cl_{09} are the chloride concentrations at S10 and S09 and Cl_{sw} is the chloride concentration of standard seawater (19,353 mg/kg; the corresponding sodium concentration, Na_{sw}, is 10,781 mg/kg; Millero et al., 2008).

Expressing the seawater end-member per litre (≈ 19,830 mg/L at a density of 1.0247 kg/L) would lower f by about 2% of its value, which does not affect any conclusion. Concentrations expected from conservative mixing were compared with those measured at S10. The model assumes that chloride gained between S09 and S10 is entirely marine and that S09 on the sampling day represents the river water reaching the lagoon. Both assumptions are tested below with the Na:Cl ratio. The model also neglects freshwater entering from the 238.9 km² catchment between S09 and S10. It is therefore used to bound the contribution of seawater dilution, not to quantify removal.

Comparison with water-quality criteria. Observations were screened against three sets of criteria, chosen for different purposes:

- The Central Pollution Control Board (CPCB) designated-best-use criteria for Class C, a drinking-water source after conventional treatment and disinfection (CPCB, n.d.), as the national reference for this use

of the river.

- The Indian drinking-water specification IS 10500:2012, reaffirmed in 2023 and including Amendments No. 1–4 (BIS, 2012). This applies to drinking water as supplied and was used here only as a reference scale for untreated river water.
- United States Environmental Protection Agency (USEPA) recreational criteria for *E. coli*, a geometric mean of 126 and a statistical threshold value (STV) of 410 per 100 mL (USEPA, 2012), and the USEPA chronic aquatic-life criterion for total ammonia-N (USEPA, 2013). These are not Indian standards and were used for comparative screening only.

The USEPA recreational criteria apply to any 30-day interval and the ammonia criterion to 30-day averages. With one sample per month, the comparisons are indicative rather than formal compliance assessments.

Use of AI-assisted tools

The Python code used for data processing, statistical analysis and figures was written and executed with the assistance of Claude (Anthropic), under the direction of the authors. The laboratory values in the master dataset were checked by the authors against the signed laboratory reports. All figures are plots generated by this code from the measured data; no generative AI imagery was used. During revision, the complete analysis was re-executed from the master dataset in a separate Python environment (see Data analysis), and it reproduced the original outputs to rounding precision. Claude and ChatGPT (OpenAI) were also used for language editing, manuscript organisation and critical review of the presentation of methods and statistical reporting. The authors take full responsibility for the analyses, the text and its conclusions. No AI tool was used as an author or as a substitute for the authors' scientific judgement.

Results

Hydrological context and its uncertainty

The campaigns covered a wide range of antecedent conditions (Fig. 4a). No rain fell in the 30 days before the January and February 2026 campaigns. In contrast, the September 2025 campaign followed 332 mm of catchment rainfall over 30 days, and the August 2026 campaign followed 107 mm in the preceding week. The June 2026 campaign followed 71 mm in the week after a near-dry spring and was the first campaign after heavy monsoon rain. The mid-monsoon July campaign followed only 8 mm. Calendar-season labels therefore did not consistently represent hydrological conditions at the time of sampling.

Modelled discharge was a weak guide at the daily scale. At the Kasipatnam gauge (2008–2011), daily skill was low before correction (KGE = 0.18, NSE = 0.14, r = 0.38) and after it (KGE = 0.28, NSE = 0.03). The corrected P10–P90 band contained only 18% of observed days against a nominal 80%, showing that the bootstrap band understates the true uncertainty. Monthly means were reproduced better (corrected KGE = 0.76, NSE = 0.56, r = 0.79, percentage bias − 11%; Online Resource 1). The campaign values are 7-day means, which lie between these two scales, and their skill was not evaluated directly.

Estimated 7-day mean discharge at S03 (P50) was 20.8 and 17.0 $m^3 s^{-1}$ before the September and October 2025 campaigns, 16.4 $m^3 s^{-1}$ before the September 2026 campaign, 5.1 $m^3 s^{-1}$ before the August 2026 campaign, and 0.7–2.0 $m^3 s^{-1}$ from December 2025 to June 2026. The June 2026 value is the least reliable, because the model underestimated June flow at Kasipatnam (2001–2011 June mean 2.4 $m^3 s^{-1}$ modelled against 7.9 $m^3 s^{-1}$ observed). Below the reservoir, the estimates depended strongly on the assumed release; for S06 before the September 2025 campaign, they ranged from 0 to 32 $m^3 s^{-1}$ across scenarios. These values are adequate only to separate the high-flow campaigns (September and October 2025, September 2026) from the dry-season campaigns.

Within stations S03–S10, dissolved ions were lower when estimated discharge was higher. The median Spearman ρ across the eight stations was − 0.71 for potassium, − 0.66 for chloride and total alkalinity, − 0.65 for sulphate and total hardness, − 0.64 for sodium and − 0.61 for TDS. For each of these, ρ was below − 0.5 at 6–8 of the 8 stations. Nutrients, BOD, COD, DO, TSS, turbidity and *E. coli* showed no consistent association. Modelled discharge is driven by the same rainfall used in the next section, and the stations are nested, so this result agrees with, but does not independently confirm, the dilution pattern seen against catchment rainfall.

Longitudinal gradient

Station effects were strong and consistent across campaigns. In the Friedman tests, most determinands with non-degenerate data showed a station effect at $p < 0.001$. Kendall's W for these determinands ranged from 0.63 (iron) to 1.00 (chloride; Online Resource 2). Lead showed a weaker station effect ($p = 0.013$, $W = 0.46$), based on the five campaigns in which all stations had detectable lead. Cadmium was not testable because all values were below the reporting limit.

Indicators of organic and faecal loading increased downstream (Table 2; Fig. 2). Median BOD increased from 0.40 mg/L at S01 to 12.25 mg/L at S09, COD from 4.0 to 55.0 mg/L, ammonia-N from 0.01 to 1.93 mg/L, and *E. coli* from 12.5 to 3,239 MPN/100 mL. The corresponding geometric means of *E. coli* were 12 and 3,136 MPN/100 mL.

Most of the change occurred below the reservoir (Table 3):

- Between S06 and S07, the catchment gained 424 km^2, including 89.5 km^2 of cropland and 17.9 km^2 of built area, and median BOD increased by 2.85 mg/L.
- Between S07 and S08, median *E. coli* increased by 1,592.5 MPN/100 mL, the largest increment for this indicator.
- Between S08 and S09, the added catchment was only 218 km^2, yet median BOD increased by 4.00 mg/L and ammonia-N by 0.68 mg/L, the largest increments for these determinands.

Across the reservoir reach (S05–S06), median BOD and TSS declined. Conservative ions increased gradually to S09 and then sharply at S10 (median chloride 51 and 208 mg/L, respectively), whereas BOD, COD, ammonia-N and *E. coli* were lower at S10 than at S09.

At station level (n = 10 nested catchments), medians of BOD, ammonia-N, chloride and *E. coli* were strongly associated with catchment area (ρ = 0.92–0.98). They were less strongly associated with crop and built-up cover (ρ = 0.54–0.60, below the nominal critical value of 0.648). The coefficients are identical for the two cover types because crop and built-up shares have the same rank order across the ten catchments. Because catchment area, cropland and built-up area all increase downstream together, these coefficients cannot separate land-use effects from the accumulation of inputs along the river.

DO ranged from 2.78 to 8.99 mg/L. It fell below the Class C minimum of 4 mg/L in four observations, at S09 in April, June and July 2026 and at S10 in October 2025. Expressed as saturation, DO showed a clear longitudinal gradient (Fig. 3). Station medians were 99% at the headwater, 95–96% in the reservoir reach, 87% at S07, 76% at S08 and 63% at S09, with a minimum of 34% at S09. Saturation was higher at the estuary (median 76%). Across station medians (n = 10), DO saturation was inversely associated with BOD (ρ = −1.00) and ammonia-N (ρ = −0.95).

Table 2
Station medians over usable campaigns (mg/L unless stated) and median and geometric mean (GM) of *Escherichia coli* (MPN/100 mL). n = 12 campaigns for laboratory determinands and 13 for DO.

Station	DO (mg/L)	DO sat. (%)	BOD	COD	NH_3-N	NH_3-N/DIN (%)	TP	TSS	Cl	*E. coli* median	*E. coli* GM
S01	8.00	99	0.40	4.0	0.01	13	0.05	14.5	5.0	12.5	12
S02	8.11	98	0.90	5.0	0.05	6	0.07	29.0	8.5	61.5	58
S03	8.01	97	1.10	7.0	0.10	12	0.21	34.5	15.5	177.5	173
S04	7.75	95	1.80	9.5	0.17	15	0.41	40.5	20.5	295.5	270
S05	7.87	95	1.75	9.0	0.18	16	0.39	34.5	19.0	421	418
S06	7.92	96	1.70	9.0	0.18	16	0.24	24.0	20.5	482	465
S07	7.15	87	4.55	18.5	0.70	57	0.47	42.0	28.5	1,033.5	1,036
S08	6.09	76	8.25	38.5	1.25	67	0.47	52.5	41.5	2,626	2,504
S09	5.16	63	12.25	55.0	1.93	76	0.50	50.0	51.0	3,239	3,136
S10	6.13	76	6.85	41.5	1.46	75	0.27	41.5	208.0	2,552.5	2,428

DIN, dissolved inorganic nitrogen (NH_3-N + NO_3-N). NH_3-N/DIN is the median of per-observation percentages. Censored values were excluded.

Table 3
Area and land cover added between consecutive stations, and the change in station medians across each reach (mg/L; *E. coli* MPN/100 mL, change in medians).

Reach	Added area (km²)	Added crops (km²)	Added built (km²)	Δ BOD	Δ NH_3-N	Δ *E. coli*	Δ TSS
S01–S02	80.5	1.8	0.5	0.50	0.04	49	14.5
S02–S03	94.5	1.1	0.7	0.20	0.04	116	5.5
S03–S04	13.5	0.1	0.1	0.70	0.08	118	6.0
S04–S05	4.5	0.0	0.0	−0.05	0.01	125.5	−6.0
S05–S06	78.3	0.6	0.3	−0.05	0.00	61	−10.5
S06–S07	423.9	89.5	17.9	2.85	0.52	551.5	18.0
S07–S08	356.7	88.1	20.1	3.70	0.55	1,592.5	10.5
S08–S09	217.8	47.5	12.8	4.00	0.68	613	−2.5
S09–S10	238.9	79.0	29.4	−5.40	−0.47	−686.5	−8.5

Differences between station medians, calculated from unrounded values; small differences from Table 2 reflect rounding. Land cover from Dynamic World (January–March 2026). Catchments are nested, so reach values are increments, not independent samples.

Rainfall-associated variation within stations

The downstream BOD gradient was present in every campaign: BOD at S01 remained below 1 mg/L, whereas BOD at S09 exceeded 10 mg/L in every usable campaign, in dry-season and monsoon campaigns alike (Fig. 4c). Median BOD at S09 was 11.8, 13.5 and 13.9 mg/L in the dry season, north-east monsoon and south-west monsoon, respectively. Campaign-to-campaign variation within stations was nevertheless associated with antecedent rainfall (Table 4; Fig. 4).

TSS, iron, TP, COD and BOD were positively associated with rainfall in the preceding week, with pooled within-station $\rho = 0.80$, 0.89, 0.71, 0.67 and 0.57, respectively. Dissolved constituents were negatively associated with rainfall, most strongly over the preceding 30 days (EC and total hardness, $\rho = -0.89$; fluoride, $\rho = -0.76$). All stations share the same 12–13 campaign conditions, so the information on temporal association comes from at most 12–13 independent conditions, not from 120 observations.

No significance test of these associations was performed, because 12–13 shared campaigns are too few to support inference on many determinand–rainfall combinations. The coefficients are therefore descriptive and exploratory. They are reported to show the direction and relative strength of the pattern: the particulate (TSS, iron) and dissolved (EC, total hardness) associations were the strongest, and the BOD association (ρ = 0.57) was the weakest and is not interpreted further.

Individual campaigns illustrate the pattern (Fig. 4):

- **June 2026.** In the first campaign after heavy monsoon rain, TSS, BOD and TP were 2.70, 1.71 and 2.10 times the station medians across the basin.
- **August 2026.** After heavier rain following a wetter July, TSS and BOD were 1.55 and 1.17 times their medians.
- **April 2026.** After 24 mm following four rainless campaigns, TSS and BOD also rose markedly at the lower stations (Fig. 4b, c).
- **Dry season.** Conductivity increased through the dry months, reaching approximately 1.7 times the station median by February, and declined as rainfall returned.

These contrasts are consistent with mobilisation of material accumulated during dry periods. However, they rest on a few individual campaigns, each a single grab sample per station. They describe concentrations at the time of sampling and are not estimates of storm loads or of continuous event dynamics.

Table 4
Within-station associations between determinands and antecedent catchment rainfall (pooled Spearman ρ of within-station ranks).

Determinand	Rainfall window	Observations / campaigns	Pooled within-station ρ
Iron	7 days	130 / 13	0.89
TSS	7 days	120 / 12	0.80
Total phosphorus	7 days	120 / 12	0.71
COD	7 days	120 / 12	0.67
BOD	7 days	120 / 12	0.57
Electrical conductivity	30 days	120 / 12	−0.89
Total hardness	30 days	120 / 12	−0.89

Rainfall is the mean of CHIRPS and IMERG V07 over each station's catchment. Coefficients are descriptive; nominal p values (all < 0.001) are not shown because they treat repeated observations at stations sharing the same campaigns as independent. Coefficients for all determinands and both windows are given in Online Resource 2.

Multivariate structure

The PCA summarises the joint structure of the dataset. Three components had eigenvalues > 1 and together explained 87.9% of the variance (48.3%, 29.1% and 10.5% after rotation; Fig. 5). The KMO measure was 0.83 (Bartlett χ^2 = 6,291, df = 190), but these statistics assume independent observations and are given descriptively.

- **VF1** loaded strongly on EC, TDS, sulphate, sodium, chloride, total hardness and total alkalinity (0.90–0.98) and moderately on potassium (0.61). It also loaded on BOD, COD, ammonia-N and *E. coli* (0.79–0.82). VF1 combines two features that both increase downstream, ion accumulation and organic–faecal loading, and so mainly represents the longitudinal gradient. Within stations it decreased with rainfall (pooled $\rho = -0.81$).
- **VF2** loaded on turbidity, TSS and iron (0.84–0.86), with a positive loading on temperature (0.74), weaker positive loadings on TP, COD and BOD (0.54–0.59), and negative loadings on DO (− 0.81) and pH (− 0.90). It was highest at S08–S09 and increased with rainfall (pooled $\rho = 0.92$), so it summarises the particulate, rainfall-linked component.
- **VF3** was dominated by nitrate (0.93), with a secondary loading on TP (0.55), and reflected a mid-basin nitrate maximum (median 4.30 mg/L as NO_3^-, ≈ 0.97 mg/L NO_3-N, at S04).

Hierarchical clustering of station medians separated the river into two groups, S01–S06 and S07–S10 (cophenetic correlation = 0.63), which coincide with the stations above and below the Thatipudi dam. The observations are repeated measures at nested stations, and the stability of the solution under resampling was not tested. The components and clusters are therefore descriptive summaries, not identified pollution sources. All loadings are given in Online Resource 2.

Nitrogen, phosphorus, fluoride and iron

The form of inorganic nitrogen changed abruptly below the reservoir. Ammonia-N formed 6–16% of DIN from S02 to S06, but 57% at S07, 67% at S08, and 76% and 75% at S09 and S10, respectively (Table 2; Fig. 6a). Median TP increased from 0.05–0.07 mg/L at S01–S02 to 0.47–0.50 mg/L at S07–S09. The median un-ionised fraction of ammonia was 2.2–5.9% across stations, giving median un-ionised ammonia-N of 0.043 mg/L at S09 and 0.083 mg/L at S10.

The USEPA (2013) chronic criterion for total ammonia-N depends on temperature and pH. The commonly quoted 1.9 mg/L applies only at pH 7 and 20°C. For any water temperature between 20 and 32°C, the un-ionised fractions observed here (2.2–5.9%) correspond to pH values at which the criterion is 0.45–1.07 mg/L. Total ammonia-N exceeded 1.9 mg/L in 13 observations, all at S08–S10. The station medians at S08–S10 (1.25–1.93 mg/L) exceed the criterion across that whole range of conditions, so the number of observations above the condition-specific criterion is larger than 13; it was not calculated for individual observations. Because the criterion refers to 30-day averages, single grab samples provide only a screening comparison.

Fluoride (as F) exceeded 1.0 mg/L in 15 of 120 observations, 14 of them between November 2025 and March 2026, but never exceeded 1.5 mg/L (Fig. 6c). It decreased with rainfall ($\rho = -0.76$). Iron exceeded the acceptable limit of 1.0 mg/L in 75 of 130 observations, at every station, and 0.3 mg/L (the acceptable limit

before Amendment No. 1) in 123 of 130. Iron increased with TSS in the observations for which both were available (July 2026 TSS excluded), but a linear regression described the relationship only loosely (slope 60.7 mg Fe per g TSS, intercept 0.005 mg/L, $R^2 = 0.46$; Fig. 6b). The scatter shows two groups of observations in which iron differs about fivefold at similar TSS; their origin was not established, and the regression is therefore given only as a rough summary.

Change between the last riverine station and the estuary

At S10, the Na:Cl mass ratio (median of per-campaign values 0.86) was well above the seawater value of 0.557 and, in 10 of the 12 campaigns, also above the ratio at S09 on the same date (median 0.84; Fig. 7). Mixing of S09 river water with seawater alone cannot produce a ratio outside the range of its two end-members. In those campaigns, therefore, at least one additional, non-marine source of sodium, and possibly of chloride, entered between S09 and S10. Possible sources include wastewater and saline groundwater; the present data cannot distinguish between them.

Attributing all of the chloride gain to seawater gives a seawater share of 0.59–1.68% at S10 (median 0.84%), highest in the dry-season campaigns. If part of the chloride is non-marine, the true seawater share is lower still. Mixing at this level would reduce the concentration of a river-borne constituent by less than 2%. Sodium was a median 1.40 times the value expected from mixing (range 1.19–1.78) and exceeded that expectation in every campaign, consistent with the additional source.

Concentrations of non-conservative constituents were lower at S10 than at S09 (Table 5). Per-campaign S10:S09 ratios had medians of 0.54 for BOD and TP, 0.77 for ammonia-N and *E. coli*, and 0.79 for TSS, against 0.99 expected from seawater mixing. Seawater dilution therefore explains almost none of the difference.

Freshwater from the 238.9 km² catchment between S09 and S10 was not measured, so its effect was bounded with a simple scenario. Assume runoff proportional to catchment area and inflow containing none of the constituent (the most favourable case for dilution). Lateral inflow would then equal 18–24% of the S09 flow, depending on whether the dam-controlled area is included, and would reduce concentrations to 0.81–0.85 of the S09 values.

- Under this scenario, the observed ratios for ammonia-N, *E. coli* and TSS (0.77–0.79) would require lateral inflow of 27–30% of the S09 flow. This is close to the scenario range, so dilution alone could account for a substantial part of these reductions.
- The ratios for BOD and TP (0.54) would require lateral inflow of about 85% of the S09 flow. This is well beyond the area-based estimate, even before allowing for the fact that this sub-catchment contains the largest built-up area added in any reach (29.4 km²) and is unlikely to supply clean water.

The scenario depends on assumed runoff and dam operation and does not account for residence time in the lagoon, so it is indicative only.

Table 5
Change between the last riverine station (S09) and the estuary (S10), compared with the change expected from seawater mixing alone at the chloride-derived seawater share and with an illustrative freshwater-dilution scenario.

Constituent	S09 median	S10 median	S10/S09 observed	Expected from seawater mixing	Lateral inflow (% of S09 flow) needed if dilution alone[a]
Chloride (mg/L)	51.0	208.0	— (tracer)	—	—
Sodium (mg/L)	40.1	189.7	4.81	3.25	—
BOD (mg/L)	12.25	6.85	0.54	0.99	85
Total phosphorus (mg/L)	0.50	0.27	0.54	0.99	85
Ammonia-N (mg/L)	1.93	1.46	0.77	0.99	30
E. coli (MPN/100 mL)	3,239	2,552.5	0.77	0.99	30
TSS (mg/L)	50.0	41.5	0.79	0.99	27
Seawater share (%)	—	0.84	range 0.59–1.68	—	—

Seawater end-members from Millero et al. (2008). Observed ratios are medians of per-campaign ratios; station medians are given for reference. *E. coli* values are medians (geometric means in Table 2). Expected ratios assume conservative mixing at the median seawater share f = 0.84%, i.e. $(1 - f) + f \cdot C_{sw}/C_{S09}$ (from Eq. 1), with C_{sw} taken as negligible for BOD, TP, ammonia-N, *E. coli* and TSS. [a]Inflow with zero concentration required to produce the observed ratio, 1/ratio − 1. Area-proportional runoff gives 18% (relative to the whole S09 catchment) to 24% (relative to the S09 catchment below the dam).

Trace metals

Arsenic was detected in every observation (0.0007–0.0080 mg/L) and lead in 102 of 130 observations (maximum 0.0086 mg/L). Cadmium was below the reporting limit of 0.0005 mg/L in every observation, and no metal reached its IS 10500 limit. Arsenic and lead showed no downstream gradient. Both increased with rainfall (pooled within-station ρ = 0.87 and 0.93, respectively), closely tracked iron across observations (ρ = 0.99 and 0.98, respectively), and reached their maxima at S01 during the wettest campaign.

Comparison with water-quality criteria

National river-use criteria (CPCB Class C). As a screening comparison (BOD measured over 3 days at 27°C; the criterion is stated for 5 days at 20°C), BOD exceeded the Class C criterion of 3 mg/L in 50 of 120 usable observations: in all 48 at S07–S10, and in two at S04 and S05. DO was below 4 mg/L in 4 of 130 observations, and pH remained within the Class C range at all stations (Table 6). The Class C criterion for

total coliforms (≤ 5,000 MPN/100 mL) could not be assessed because total coliforms were not measured. *E. coli* concentrations below 5,000 MPN/100 mL do not imply compliance with it.

Bathing use (CPCB Class B). Total coliform counts are at least as high as *E. coli* counts. The *E. coli* results therefore show that the Class B criterion for organised outdoor bathing (total coliforms ≤ 500 MPN/100 mL) was not met at S07–S10: the geometric mean *E. coli* exceeded 500 MPN/100 mL at all four stations, and all 48 individual observations at S07–S10 exceeded 500 MPN/100 mL.

Drinking-water specification (IS 10500:2012, reference scale only). E. coli was detected in every observation and turbidity exceeded the permissible limit of 5 NTU in every observation. Ammonia-N exceeded 0.5 mg/L in 48 observations, all at S07–S10, and fluoride exceeded the acceptable limit of 1.0 mg/L in 15 observations. TDS exceeded the acceptable limit of 500 mg/L in 11 observations, all at S10, and iron exceeded the acceptable limit of 1.0 mg/L in 75 of 130 observations. Manganese, which the standard also limits jointly with iron, was not measured. These comparisons describe the treatment burden of the raw water and are not assessments of supplied drinking water.

USEPA recreational criteria (comparative screening). The geometric mean of *E. coli* over the 12 campaigns was below 126 per 100 mL only at S01 and S02. It was 1,036 at S07 and 2,428–3,136 at S08–S10, i.e. 8–25 times the value. *E. coli* exceeded the STV of 410 per 100 mL in every usable campaign from S07 to the estuary. These comparisons are based on monthly single samples rather than the 30-day sampling frame of the criteria. They use MPN counts rather than the membrane-filtration counts on which the criteria were based, so they indicate the order of magnitude of exceedance rather than formal non-attainment.

Table 6
Screening of station-campaign observations against national criteria (CPCB Class C; IS 10500:2012 with Amendments No. 1–4), as number of observations exceeding the value out of usable observations.

Criterion	Determinand and value	Type of value	Exceedances	Stations
CPCB Class C	BOD > 3 mg/L	Maximum	50/120	S04, S05, S07–S10
CPCB Class C	DO < 4 mg/L	Minimum	4/130	S09, S10
CPCB Class C	Total coliforms > 5,000 MPN/100 mL	Maximum	Not assessed (not measured)	—
IS 10500	Ammonia (total ammonia-N) > 0.5 mg/L	Acceptable	48/120	S07–S10
IS 10500	Fluoride > 1.0 mg/L	Acceptable (permissible 1.5)	15/120	S04, S05, S07, S09, S10
IS 10500	Iron > 1.0 mg/L	Acceptable (Amendment No. 1, 2015)	75/130	All
IS 10500	Turbidity > 5 NTU	Permissible (acceptable 1)	120/120	All
IS 10500	TDS > 500 mg/L	Acceptable (permissible 2,000)	11/120	S10
IS 10500	*E. coli* detectable in 100 mL	Not detectable	120/120	All

IS 10500 applies to drinking water as supplied; values for untreated river water are given as a reference scale only. No observation exceeded the IS 10500 limits for arsenic, cadmium, lead, nitrate or sulphate, or fell outside the Class C pH range, and fluoride never exceeded 1.5 mg/L. Censored values were excluded. BOD was measured as BOD_3 at 27°C, whereas the CPCB criterion is stated for BOD_5 at 20°C (see Methods).

Discussion

The findings fall into three levels of evidence, summarised in Table 7: patterns observed directly, interpretations consistent with them, and mechanisms that remain unresolved. The discussion follows the same order.

Where the deterioration occurs and why it points to wastewater-associated loading

The strongest and most robust result is spatial. Organic and faecal indicators, ammonia-N and DO saturation changed little from S01 to S06 and deteriorated steeply from S06 to S09. This ordering was consistent enough across campaigns to give strong Friedman station effects, and BOD exceeded the national Class C criterion (screening comparison, BOD_3 at 27°C) in every usable campaign at S07–S10.

Three features of the observations are consistent with domestic wastewater-associated loading below the reservoir:

- BOD, ammonia-N, *E. coli* and TP increased together in reaches containing towns and larger villages. The largest BOD and ammonia increments occurred where a relatively small added area (S08–S09) contained substantial settlement.
- Reduced nitrogen dominated where these indicators were highest. Ammonia-N formed 57–76% of DIN below the reservoir compared with 6–16% above it, a pattern similar to that of wastewater-affected rivers such as the Bagmati below Kathmandu (Bhatt et al., 2014).
- The BOD gradient was present in dry-season and monsoon campaigns alike, which suggests a persistent input rather than one generated only by rainfall.

Untreated sewage entering the river, and washing and bathing in it, were seen during fieldwork, although not recorded systematically by reach. These observations support a wastewater-associated interpretation but do not constitute source tracking. No wastewater-specific tracers, outfall inventory or discharge measurements were available. Livestock, agricultural runoff, reduced dilution below the dam and in-stream processes may all contribute, and their relative shares cannot be estimated from this design. The nested catchments also mean that the association with built-up and crop cover cannot be separated from accumulation along the river.

The oxygen regime is consistent with sustained organic loading. Median DO saturation declined from 99% at the headwater to 63% at S09, and across stations it closely tracked BOD and ammonia-N. This pattern is compatible with oxygen consumption by organic and nitrogenous demand (Streeter & Phelps, 1925). DO fell below 4 mg/L at S09 in three campaigns. Below a reservoir from which water is abstracted for supply, dilution in the dry season may be limited, and warming would be expected to increase oxygen demand relative to reaeration (Chapra et al., 2021); river temperatures in several Indian basins are projected to rise (Rehana & Rajesh, 2023). Single grab samples do not resolve the diurnal DO cycle, so the daily minimum DO at the lower stations may have been lower than the values recorded. Unlike the Musi below Hyderabad, where water quality improved downstream of wastewater discharge (Ensink et al., 2010), the Gosthani showed no comparable recovery: organic and faecal indicators were still increasing at S09, approximately 12 km upstream of the estuary.

Reach-by-reach context

In the upper basin (S01–S03), trees cover 57–77% of the catchments and built area is 1.2% or less (Table 1). S01 was the least affected station, even though its catchment contains Katiki waterfall, where intense visitor use and many macaques fed by visitors were noted during the campaigns. The geometric mean of *E. coli* rose from 12 MPN/100 mL at S01 to 58 at S02, below the Borra Caves, and 173 at S03, and median BOD rose from 0.40 to 0.90 mg/L at S02. These increases are small in absolute terms. They may reflect a diluted tourism-related or animal input, but *E. coli* cannot distinguish human from animal faecal contamination (Harwood et al., 2014). S03 lies beside a toll gate on the main road. Median TSS rose only

from 29.0 to 34.5 mg/L between S02 and S03 and median lead did not rise (0.0032 and 0.0028 mg/L), so the data show no clear road-runoff signal.

Between S03 and S04, above the reservoir, median BOD rose from 1.10 to 1.80 mg/L and TP from 0.21 to 0.41 mg/L, although the catchment gained only 13.5 km². This points to a local input near S04 rather than a diffuse one; the input was not identified. Cropland makes up only about 2% of these catchments, so arable runoff is an unlikely main source of the nitrate maximum at S04–S06 (medians 4.24–4.30 mg/L as NO_3^-). Village sanitation, livestock and nitrification in the forested, carbonate-bearing upper catchment are plausible alternatives that were not examined. Across the reservoir the pattern reversed: from S05 to S06, median TSS fell from 34.5 to 24.0 mg/L and TP from 0.39 to 0.24 mg/L, as expected where a reservoir traps sediment and particle-bound phosphorus, while DO changed little (7.87 and 7.92 mg/L).

Below the dam, the largest increments coincided with the entry of cropland and built area (Table 3). Between S06 and S07, BOD, ammonia-N and median *E. coli* rose together (by 2.85 mg/L, 0.52 mg/L and 551.5 MPN/100 mL), a combination expected of domestic wastewater. This reach includes the towns of Srungavarapukota and Lakkavarapukota. The steepest rise in *E. coli* occurred between S07 and S08, and the largest BOD and ammonia-N increments between S08 and S09, a 218 km² reach between the Bhimasingi and Pandrangi bridges. Median TSS rose from 24.0 to 52.5 mg/L between S06 and S08 and did not rise further at S09 (50.0 mg/L). This is consistent with runoff from agricultural land or roads but cannot be attributed with the present data.

Rainfall and the particulate signal

Rainfall was associated mainly with the particulate component of the signal and with dilution of dissolved constituents. It was not associated with the persistent organic and faecal gradient, whose rank order between stations was maintained in dry-season and monsoon campaigns alike. The TSS, iron and conductivity associations were the strongest and the BOD association the weakest; none was formally tested, and all are treated as exploratory.

The June 2026 campaign, the first after heavy monsoon rain, showed larger relative increases in TSS and BOD than the August campaign, which followed heavier rain in a wetter period. The April campaign, after modest rain following a long dry spell, also showed elevated TSS and BOD at the lower stations. These contrasts are consistent with mobilisation of particulate and organic material accumulated during dry periods, as reported for early-monsoon events elsewhere in the tropics (Huon et al., 2017). They rest on individual campaigns with single samples, however. They do not demonstrate a general first-flush effect (Bertrand-Krajewski et al., 1998; Bach et al., 2010; Gao et al., 2023), and they cannot separate the effect of storm timing from that of sampling time relative to the hydrograph.

The practical implication is that the timing of fixed monthly sampling relative to rainfall can change the concentrations recorded by a factor of about two to three. Monitoring designs for such rivers should therefore record antecedent rainfall and include targeted event sampling.

What modelled discharge can and cannot show

Modelled discharge added little independent information. Its daily skill at the only gauge was poor (corrected NSE = 0.03), its uncertainty band captured only 18% of observed days, its skill at the 7-day scale used for the campaigns is unknown, and below the dam it depends on unrecorded releases. The negative association between estimated discharge and dissolved ions is consistent with dilution, but it is not independent confirmation, because the model is forced by the same rainfall. The data do not support estimates of pollutant loads or fluxes. They cannot separate the effects of added inputs and reduced dilution below the reservoir, nor show whether the lower concentrations at S10 reflect a loss of mass.

What the estuarine comparison establishes

The chloride and sodium data establish two points. First, seawater dilution at S10 was negligible (< 2%). Second, the two-end-member assumption is incomplete, because S10 received an additional non-marine sodium source.

The lower concentrations at S10 must therefore reflect freshwater dilution from the coastal sub-catchment, in-lagoon processes, differences in the timing of the water sampled, or a combination of these. For ammonia-N, *E. coli* and TSS, the reductions are of a size that unmeasured lateral inflow could largely produce. For BOD and TP, the reductions (about 46%) exceed what area-proportional dilution by clean water could produce. This is consistent with possible attenuation within the lagoon, but the volume and composition of lateral inflow and the residence time of the lagoon were not measured, so attenuation cannot be confirmed.

Plausible mechanisms include settling of particles and particle-associated phosphorus and organic matter, bacterial die-off in brackish, sunlit water (Rozen & Belkin, 2001) and ammonium transformation at low salinity (Cheong et al., 2024). None was measured. The results therefore show a concentration change between S09 and S10, not a demonstrated removal mechanism or a net reduction in pollutant mass. If retention occurs, it could increase the exposure of lagoon sediments and bivalves to contaminants; neither was sampled.

Coastal health and the bivalve fishery

The faecal contamination measured in the lower river is relevant to the receiving lagoon, which is used for bathing and bivalve harvesting. Non-consumptive domestic contact with surface water is also a recognised exposure route in rural India (Daniels et al., 2023). The geometric mean *E. coli* at S07–S10 was approximately 1,000–3,100 MPN/100 mL. The coastal waters receiving the river have previously been reported to contain indicator and pathogenic bacteria above standard limits (Sudha Rani et al., 2018). Recreational criteria are based on specific exposure assumptions and sampling frequencies (Wiedenmann et al., 2006; Russo et al., 2020), so the comparisons here are screening-level rather than estimates of illness risk. Nevertheless, the magnitude of the observed concentrations, consistently above the national bathing criterion at S07–S10, supports continued microbiological monitoring of the lower river and estuary. Testing for antimicrobial resistance would be a logical next step, given reports of resistant *E. coli* in Indian aquatic environments (Diwan et al., 2018; Maloo et al., 2017).

Trace metals and geogenic constituents

Arsenic and lead were present at low concentrations and cadmium was not detected. Their lack of a downstream increase, their increase after rainfall and their association with iron are consistent with predominantly particulate transport from weathered lateritic soils (Nasrabadi et al., 2016) rather than a strong localised source in the lower basin. No enrichment was evident in lower-basin reaches containing brick kilns, although brick-kiln areas elsewhere have been associated with trace-metal contamination (Kumar et al., 2021; Haque et al., 2022). Because particle-bound metals can settle in low-energy estuarine environments, sediment and bivalve sampling would be needed to determine whether the lagoon accumulates them.

Not every exceedance was necessarily anthropogenic. Fluoride increased through the dry season, when groundwater sustains flow, consistent with geogenic fluoride reported in the region (Subba Rao, 2009; Podgorski et al., 2018). Iron was associated with suspended particles, consistent with particulate and colloidal iron transport in tropical rivers (Allard et al., 2004). These constituents matter for drinking-water treatment but do not alter the evidence for a sanitation-related signal in the lower basin.

Contribution to monitoring and management

The study provides a full-year, ten-station baseline for a river that is not routinely monitored. It locates the main deterioration in the 30 km below the Thatipudi dam and shows that BOD in this reach exceeded the national Class C value in every usable campaign (screening comparison). For monitoring, three points follow:

- A small number of stations (S06, S07, S09 and S10) would capture the main gradient and the estuarine transition.
- Ammonia-N and *E. coli* together distinguished the lower river more clearly than any single indicator.
- Rainfall timing must be recorded and, ideally, paired with discharge gauging if loads are to be estimated.

Limitations

- **Hydrology.** Discharge was not measured. Modelled discharge is reliable only at monthly to seasonal scale, was calibrated only at S03 against 2001–2011 records, was not estimated for S01 and S02, and below the reservoir depended on assumed releases. Loads and the relative roles of added inputs and reduced dilution therefore cannot be determined.
- **Sampling design.** Each station was sampled once per month with a single grab sample. Short-lived events were captured only when they coincided with a campaign, and diurnal variation in DO was not controlled.
- **Temporal inference.** All stations share the same 12–13 sampling conditions, so temporal associations rest on 12–13 independent conditions and are exploratory.
- **Nested catchments.** With ten nested catchments, land-use effects cannot be statistically separated from downstream accumulation.

- **Laboratory QA/QC.** Batch-level QA/QC data were not available, so the precision and bias of individual results are unknown. The July 2026 laboratory results were excluded, leaving 12 campaigns for most determinands and an annual summary weighted towards September. BOD was measured as BOD_3 at 27°C, so comparisons with criteria stated for BOD_5 at 20°C are approximate.
- **Statistical inference.** Rainfall associations, catchment-attribute correlations and the multivariate analyses are exploratory; no permutation-based or other dependence-aware test of the rainfall associations was performed, and the stability of the PCA was not assessed.
- **Estuarine comparison.** The S09–S10 comparison does not include the freshwater or wastewater entering the lagoon from its own sub-catchment.

Table 7
Summary of findings by level of evidence.

Level	Finding	Basis	What would strengthen it
Directly observed	Steep downstream increase in BOD, COD, ammonia-N, TP and *E. coli*, and decrease in DO saturation, concentrated below the Thatipudi dam	Station medians; Friedman tests with campaign as block	Batch QA/QC; continued monitoring
Directly observed	BOD_3 > 3 mg/L in all 48 usable observations at S07–S10 (screening against a BOD_5 criterion)	Individual observations	Paired $BOD_{3,27}$ and $BOD_{5,20}$ measurements
Directly observed	Ammonia-N dominates DIN below the dam	Station medians	—
Directly observed	Seawater share at S10 < 2%; Na:Cl at S10 outside the river–seawater range in 10 of 12 campaigns; sodium above the mixing expectation in all 12	Chloride and sodium balance	Salinity profiles; lagoon sampling
Supported interpretation	Pattern consistent with domestic wastewater-associated loading	Co-variation of indicators, nitrogen speciation, persistence across seasons, field observations	Outfall inventory; human-specific markers; wastewater tracers
Supported interpretation	Rainfall associated with higher particulate and lower dissolved concentrations	Within-station rank correlations (12–13 campaigns; not formally tested)	Event sampling; campaign-level permutation tests
Supported interpretation	BOD and TP decreases between S09 and S10 larger than plausible dilution, consistent with possible attenuation in the lagoon	Mixing calculation plus area-based dilution scenario	Discharge and lateral-inflow measurements; sediment sampling
Unresolved	Relative contributions of sources; role of reduced dilution below the dam	—	Discharge gauging; reach-by-reach source survey; source apportionment
Unresolved	Mechanisms of change in the lagoon; net change in mass	—	Flow and residence-time measurements; sediment and bivalve analyses

Conclusions

Thirteen monthly campaigns at ten stations located where the Gosthani River deteriorates. Water quality was nearly unchanged from the forested headwater to the Thatipudi dam. Organic and faecal indicators then rose steeply over the next 30 km, with the largest increments in two reaches that contain towns and

villages. The contrast between the upper and the lower river was present in every sampled campaign. In a screening comparison, BOD exceeded the national Class C value in every usable campaign at the four downstream stations, and ammonia-N formed most of the inorganic nitrogen there.

For monitoring, a small set of stations (below the dam, two lower-river bridges and the estuary) would capture the gradient and the estuarine transition. Ammonia-N and *E. coli* together separated the affected reaches most clearly. Fixed monthly sampling recorded concentrations that varied with antecedent rainfall, so rainfall at the time of sampling should be documented. These rainfall associations rest on 12–13 shared campaigns and remain exploratory.

The composition of the downstream signal is consistent with domestic wastewater-associated loading, but this study did not apportion sources. The decrease in concentrations between the last riverine station and the estuary could not be separated from unmeasured lateral inflow for most constituents. Discharge gauging, event-based sampling and source-specific indicators would be needed to quantify loads, attribute them to sources and determine what the lagoon retains.

Statements and Declarations

Acknowledgements

The authors thank the laboratories that carried out the analyses and the residents of the Gosthani basin who assisted during fieldwork.

Funding

This research received no specific grant from any funding agency in the public, commercial, or not-for-profit sectors.

Competing interests

The authors declare no competing financial or non-financial interests that could have influenced the work reported in this paper.

Ethics approval

This study did not involve human participants or animals; ethics approval and consent were therefore not applicable.

Consent to participate

Not applicable.

Consent for publication

Not applicable.

Data and code availability

The station-by-campaign dataset, delineated catchments and analysis scripts are available from the corresponding author on reasonable request. The modelled discharge estimates, their calibration statistics and the associated correlations are provided as Online Resource 1. Station summaries, test statistics, rainfall correlations for all determinands and PCA loadings are provided as Online Resource 2.

Author contributions

Mohammad Mdhour Ahmad Abuqrian: Conceptualization, Methodology, Investigation, Formal analysis, Data curation, Visualization, Writing – original draft. B. Vijaya Saradhi: Supervision, Conceptualization, Writing – review & editing.

Ethical responsibilities of authors

All authors have read, understood, and have complied as applicable with the statement on “Ethical responsibilities of Authors” as found in the Instructions for Authors.

References

1. Acharyya, T., Sarma, V. V. S. S., Sridevi, B., Venkataramana, V., Bharathi, M. D., Naidu, S. A., Kumar, B. S. K., Prasad, V. R., Bandyopadhyay, D., Reddy, N. P. C., & Kumar, M. D. (2012). Reduced river discharge intensifies phytoplankton bloom in Godavari estuary, India. *Marine Chemistry*, *132–133*, 15–22. https://doi.org/10.1016/j.marchem.2012.01.005
2. Acharyya, T., Sudatta, B. P., Srichandan, S., Baliarsingh, S. K., Lotliker, A. A., Raulo, S., Singh, S., & Samanta, A. (2021). Deciphering long-term seasonal and tidal water quality trends in the Mahanadi estuary. *Journal of Coastal Conservation*, *25*(6), Article 56. https://doi.org/10.1007/s11852-021-00843-2
3. Alexander, R. B., Boyer, E. W., Smith, R. A., Schwarz, G. E., & Moore, R. B. (2007). The role of headwater streams in downstream water quality. *Journal of the American Water Resources Association*, *43*(1), 41–59. https://doi.org/10.1111/j.1752-1688.2007.00005.x
4. Allard, T., Menguy, N., Salomon, J., Calligaro, T., Weber, T., Calas, G., & Benedetti, M. F. (2004). Revealing forms of iron in river-borne material from major tropical rivers of the Amazon Basin (Brazil). *Geochimica et Cosmochimica Acta*, *68*(14), 3079–3094. https://doi.org/10.1016/j.gca.2004.01.014
5. American Public Health Association (APHA), American Water Works Association, & Water Environment Federation. (2023). *Standard Methods for the Examination of Water and Wastewater* (24th ed.). Washington, DC.
6. AP State Water. (n.d.). *Daily river discharge records, Kasipatnam gauging station, 2001–2011* [Data set]. India Water Resources Information System (India-WRIS), Ministry of Jal Shakti. https://indiawris.gov.in/wris/
7. Bach, P. M., McCarthy, D. T., & Deletic, A. (2010). Redefining the stormwater first flush phenomenon. *Water Research*, *44*(8), 2487–2498. https://doi.org/10.1016/j.watres.2010.01.022

8. Bartlett, M. S. (1950). Tests of significance in factor analysis. *British Journal of Psychology (Statistical Section)*, *3*(2), 77–85. https://doi.org/10.1111/j.2044-8317.1950.tb00285.x
9. Bertrand-Krajewski, J.-L., Chebbo, G., & Saget, A. (1998). Distribution of pollutant mass vs volume in stormwater discharges and the first flush phenomenon. *Water Research*, *32*(8), 2341–2356. https://doi.org/10.1016/S0043-1354(97)00420-X
10. Bhatt, M. P., McDowell, W. H., Gardner, K. H., & Hartmann, J. (2014). Chemistry of the heavily urbanized Bagmati River system in Kathmandu Valley, Nepal: Export of organic matter, nutrients, major ions, silica, and metals. *Environmental Earth Sciences*, *71*(2), 911–922. https://doi.org/10.1007/s12665-013-2494-9
11. Brown, C. F., Brumby, S. P., Guzder-Williams, B., Birch, T., Hyde, S. B., Mazzariello, J., Czerwinski, W., Pasquarella, V. J., Haertel, R., Ilyushchenko, S., Schwehr, K., Weisse, M., Stolle, F., Hanson, C., Guinan, O., Moore, R., & Tait, A. M. (2022). Dynamic World, Near real-time global 10 m land use land cover mapping. *Scientific Data*, *9*, 251. https://doi.org/10.1038/s41597-022-01307-4
12. Bureau of Indian Standards (BIS). (1993). *IS 3025 (Part 44): 1993 – Methods of sampling and test (physical and chemical) for water and wastewater, Part 44: Biochemical oxygen demand (BOD)* (First revision). New Delhi: BIS.
13. Bureau of Indian Standards (BIS). (2012). *IS 10500:2012 – Drinking water: Specification* (Second revision; reaffirmed 2018 and 2023; incorporating Amendment No. 1, June 2015; No. 2, September 2018; No. 3, February 2021; No. 4, November 2021). New Delhi: BIS.
14. Central Pollution Control Board (CPCB). (n.d.). *Designated best use water quality criteria for inland surface waters (Classes A to E)*. New Delhi: Ministry of Environment, Forest and Climate Change. https://cpcb.nic.in/water-quality-criteria/
15. Central Pollution Control Board. (2023). *Water quality data of medium and minor rivers 2023*. National Water Quality Monitoring Programme. https://cpcb.nic.in/wqm/2023/Water_Quality_data_of_Med_Min_River_2023.pdf
16. Central Pollution Control Board. (2022). *Polluted river stretches for restoration of water quality – 2022*. Water Quality Management (I) Division, Central Pollution Control Board, Ministry of Environment, Forest and Climate Change.
17. Chapra, S. C., Camacho, L. A., & McBride, G. B. (2021). Impact of global warming on dissolved oxygen and BOD assimilative capacity of the world's rivers: Modeling analysis. *Water*, *13*(17), 2408. https://doi.org/10.3390/w13172408
18. Cheong, A. Y. L., Annammala, K. V., Yong, E. L., Zhou, Y., Nichols, R. S., & Martin, P. (2024). Distribution of nutrients and dissolved organic matter in a eutrophic equatorial estuary: The Johor River and the East Johor Strait. *Biogeosciences*, *21*(12), 2955–2971. https://doi.org/10.5194/bg-21-2955-2024
19. Clark, A., Turner, T., Dorothy, K. P., Goutham, J., Kalavati, C., & Rajanna, B. (2003). Health hazards due to pollution of waters along the coast of Visakhapatnam, east coast of India. *Ecotoxicology and Environmental Safety*, *56*(3), 390–397. https://doi.org/10.1016/S0147-6513(03)00098-8
20. Copernicus Emergency Management Service. (n.d.). *River discharge and related historical data from the Global Flood Awareness System* [Data set]. Early Warning Data Store.

https://doi.org/10.24381/cds.a4fdd6b9

21. Daniels, M. E., Pradhan, A., Odagiri, M., & Jenkins, M. W. (2023). Waterborne exposure during non-consumptive domestic use of surface water: A population study across WASH service levels in rural India. *Journal of Water and Health*, *21*(6), 751–762. https://doi.org/10.2166/wh.2023.309
22. Diwan, V., Hanna, N., Purohit, M., Chandran, S., Riggi, E., Parashar, V., Tamhankar, A. J., & Stålsby Lundborg, C. (2018). Seasonal variations in water-quality, antibiotic residues, resistant bacteria and antibiotic resistance genes of *Escherichia coli* isolates from water and sediments of the Kshipra River in Central India. *International Journal of Environmental Research and Public Health*, *15*(6), Article 1281. https://doi.org/10.3390/ijerph15061281
23. Downing, J. A., Cole, J. J., Duarte, C. M., Middelburg, J. J., Melack, J. M., Prairie, Y. T., Kortelainen, P., Striegl, R. G., McDowell, W. H., & Tranvik, L. J. (2012). Global abundance and size distribution of streams and rivers. *Inland Waters*, *2*(4), 229–236. https://doi.org/10.5268/IW-2.4.502
24. Drusch, M., Del Bello, U., Carlier, S., Colin, O., Fernandez, V., Gascon, F., Hoersch, B., Isola, C., Laberinti, P., Martimort, P., Meygret, A., Spoto, F., Sy, O., Marchese, F., & Bargellini, P. (2012). Sentinel-2: ESA's optical high-resolution mission for GMES operational services. *Remote Sensing of Environment*, *120*, 25–36. https://doi.org/10.1016/j.rse.2011.11.026
25. Emerson, K., Russo, R. C., Lund, R. E., & Thurston, R. V. (1975). Aqueous ammonia equilibrium calculations: Effect of pH and temperature. *Journal of the Fisheries Research Board of Canada*, *32*(12), 2379–2383. https://doi.org/10.1139/f75-274
26. Ensink, J. H. J., Scott, C. A., Brooker, S., & Cairncross, S. (2010). Sewage disposal in the Musi-River, India: Water quality remediation through irrigation infrastructure. *Irrigation and Drainage Systems*, *24*(1–2), 65–77. https://doi.org/10.1007/s10795-009-9088-4
27. European Space Agency. (n.d.). *Copernicus DEM – Global and European Digital Elevation Model (COP-DEM), GLO-30* [Data set]. Produced using Copernicus WorldDEM-30 © DLR e.V. 2010–2014 and © Airbus Defence and Space GmbH 2014–2018 provided under COPERNICUS by the European Union and ESA. Earth Engine asset COPERNICUS/DEM/GLO30. https://doi.org/10.5270/ESA-c5d3d65
28. Friedman, M. (1937). The use of ranks to avoid the assumption of normality implicit in the analysis of variance. *Journal of the American Statistical Association*, *32*(200), 675–701. https://doi.org/10.1080/01621459.1937.10503522
29. Funk, C., Peterson, P., Landsfeld, M., Pedreros, D., Verdin, J., Shukla, S., Husak, G., Rowland, J., Harrison, L., Hoell, A., & Michaelsen, J. (2015). The climate hazards infrared precipitation with stations—a new environmental record for monitoring extremes. *Scientific Data*, *2*, 150066. https://doi.org/10.1038/sdata.2015.66
30. Ganesh, B., Naidu, A. G. S. S., Jagannadha Rao, M., Karuna Karudu, T., & Avatharam, P. (2013). Studies on textural characteristics of sediments from Gosthani River Estuary – Bheemunipatnam, A.P., east coast of India. *Journal of the Indian Geophysical Union*, *17*(2), 139–151.
31. Gao, Z., Zhang, Q., Li, J., Wang, Y., Dzakpasu, M., & Wang, X. C. (2023). First flush stormwater pollution in urban catchments: A review of its characterization and quantification towards optimization of

control measures. *Journal of Environmental Management*, *340*, 117976. https://doi.org/10.1016/j.jenvman.2023.117976

32. Gudmundsson, L., Bremnes, J. B., Haugen, J. E., & Engen-Skaugen, T. (2012). Technical Note: Downscaling RCM precipitation to the station scale using statistical transformations – a comparison of methods. *Hydrology and Earth System Sciences*, *16*(9), 3383–3390. https://doi.org/10.5194/hess-16-3383-2012
33. Gupta, H. V., Kling, H., Yilmaz, K. K., & Martinez, G. F. (2009). Decomposition of the mean squared error and NSE performance criteria: Implications for improving hydrological modelling. *Journal of Hydrology*, *377*(1–2), 80–91. https://doi.org/10.1016/j.jhydrol.2009.08.003
34. Haque, S. E., Shahriar, M. M., Nahar, N., & Haque, M. S. (2022). Impact of brick kiln emissions on soil quality: A case study of Ashulia brick kiln cluster, Bangladesh. *Environmental Challenges*, *9*, 100640. https://doi.org/10.1016/j.envc.2022.100640
35. Harrigan, S., Zsoter, E., Alfieri, L., Prudhomme, C., Salamon, P., Wetterhall, F., Barnard, C., Cloke, H., & Pappenberger, F. (2020). GloFAS-ERA5 operational global river discharge reanalysis 1979–present. *Earth System Science Data*, *12*(3), 2043–2060. https://doi.org/10.5194/essd-12-2043-2020
36. Harwood, V. J., Staley, C., Badgley, B. D., Borges, K., & Korajkic, A. (2014). Microbial source tracking markers for detection of fecal contamination in environmental waters: Relationships between pathogens and human health outcomes. *FEMS Microbiology Reviews*, *38*(1), 1–40. https://doi.org/10.1111/1574-6976.12031
37. Holm, S. (1979). A simple sequentially rejective multiple test procedure. *Scandinavian Journal of Statistics*, *6*(2), 65–70.
38. Huffman, G. J., Stocker, E. F., Bolvin, D. T., Nelkin, E. J., & Tan, J. (2023). *GPM IMERG Final Precipitation L3 Half Hourly 0.1 degree x 0.1 degree V07* [Data set]. NASA Goddard Earth Sciences Data and Information Services Center. Earth Engine asset NASA/GPM_L3/IMERG_V07. https://doi.org/10.5067/GPM/IMERG/3B-HH/07
39. Huon, S., Evrard, O., Gourdin, E., Lefèvre, I., Bariac, T., Reyss, J.-L., Henry des Tureaux, T., Sengtaheuanghoung, O., Ayrault, S., & Ribolzi, O. (2017). Suspended sediment source and propagation during monsoon events across nested sub-catchments with contrasted land uses in Laos. *Journal of Hydrology: Regional Studies, 9*, 69–84. https://doi.org/10.1016/j.ejrh.2016.11.018
40. Kaiser, H. F. (1958). The varimax criterion for analytic rotation in factor analysis. *Psychometrika*, *23*(3), 187–200. https://doi.org/10.1007/BF02289233
41. Kaiser, H. F. (1970). A second generation little jiffy. *Psychometrika*, *35*(4), 401–415. https://doi.org/10.1007/BF02291817
42. Krabbenhoft, C. A., Allen, G. H., Lin, P., Godsey, S. E., Allen, D. C., Burrows, R. M., DelVecchia, A. G., Fritz, K. M., Shanafield, M., Burgin, A. J., Zimmer, M. A., Datry, T., Dodds, W. K., Jones, C. N., Mims, M. C., Franklin, C., Hammond, J. C., Zipper, S., Ward, A. S., … Olden, J. D. (2022). Assessing placement bias of the global river gauge network. *Nature Sustainability*, *5*(7), 586–592. https://doi.org/10.1038/s41893-022-00873-0

43. Krishna, M. S., Prasad, M. H. K., Rao, D. B., Viswanadham, R., Sarma, V. V. S. S., & Reddy, N. P. C. (2016). Export of dissolved inorganic nutrients to the northern Indian Ocean from the Indian monsoonal rivers during discharge period. *Geochimica et Cosmochimica Acta*, *172*, 430–443. https://doi.org/10.1016/j.gca.2015.10.013

44. Kumar, S., Zhao, M., Zhang, H., Rahman, M. A., Luo, C., & Rahman, M. M. (2021). Distribution, contamination status and source of trace elements in the soil around brick kilns. *Chemosphere*, *263*, 127882. https://doi.org/10.1016/j.chemosphere.2020.127882

45. Le Bas, M. J., Subbarao, K. V., & Walsh, J. N. (2002). Metacarbonatite or marble? — The case of the carbonate, pyroxenite, calcite–apatite rock complex at Borra, Eastern Ghats, India. *Journal of Asian Earth Sciences*, *20*(2), 127–140. https://doi.org/10.1016/S1367-9120(01)00030-X

46. Lehner, B., & Grill, G. (2013). Global river hydrography and network routing: Baseline data and new approaches to study the world's large river systems. *Hydrological Processes*, *27*(15), 2171–2186. https://doi.org/10.1002/hyp.9740

47. Maloo, A., Fulke, A. B., Mulani, N., Sukumaran, S., & Ram, A. (2017). Pathogenic multiple antimicrobial resistant *Escherichia coli* serotypes in recreational waters of Mumbai, India: A potential public health risk. *Environmental Science and Pollution Research*, *24*(12), 11504–11517. https://doi.org/10.1007/s11356-017-8760-8

48. Millero, F. J., Feistel, R., Wright, D. G., & McDougall, T. J. (2008). The composition of Standard Seawater and the definition of the Reference-Composition Salinity Scale. *Deep Sea Research Part I: Oceanographic Research Papers*, *55*(1), 50–72. https://doi.org/10.1016/j.dsr.2007.10.001

49. Nash, J. E., & Sutcliffe, J. V. (1970). River flow forecasting through conceptual models part I — A discussion of principles. *Journal of Hydrology*, *10*(3), 282–290. https://doi.org/10.1016/0022-1694(70)90255-6

50. Nasrabadi, T., Ruegner, H., Sirdari, Z. Z., Schwientek, M., & Grathwohl, P. (2016). Using total suspended solids (TSS) and turbidity as proxies for evaluation of metal transport in river water. *Applied Geochemistry*, *68*, 1–9. https://doi.org/10.1016/j.apgeochem.2016.03.003

51. Pattanayak, A. A., Swain, S., Behera, R. R., Sharma, S. D., Panda, C. R., & Mohanty, P. K. (2024). Variability in water quality of two meso-tidal estuaries of Odisha, East Coast of India. *Journal of Marine Systems*, *241*, Article 103919. https://doi.org/10.1016/j.jmarsys.2023.103919

52. Podgorski, J. E., Labhasetwar, P., Saha, D., & Berg, M. (2018). Prediction modeling and mapping of groundwater fluoride contamination throughout India. *Environmental Science & Technology*, *52*(17), 9889–9898. https://doi.org/10.1021/acs.est.8b01679

53. Rama Rao, K., Jaya, P., Ratna Priya, T., Sandhya, T., Amruthavarshini, N., Sai Chaitanya, G., & Jhansi, K. (2024). Intertidal bivalve diversity and fishery of the Gosthani estuary, Bhimunipatnam, Visakhapatnam, east coast of India. *Uttar Pradesh Journal of Zoology*, *45*(11), 294–304. https://doi.org/10.56557/upjoz/2024/v45i114097

54. Rehana, S., & Rajesh, M. (2023). Assessment of impacts of climate change on Indian riverine thermal regimes using hybrid deep learning methods. *Water Resources Research, 59*(2), e2021WR031347. https://doi.org/10.1029/2021WR031347

55. Rozen, Y., & Belkin, S. (2001). Survival of enteric bacteria in seawater. *FEMS Microbiology Reviews*, *25*(5), 513–529. https://doi.org/10.1111/j.1574-6976.2001.tb00589.x

56. Ruhi, A., Messager, M. L., & Olden, J. D. (2018). Tracking the pulse of the Earth's fresh waters. *Nature Sustainability*, *1*(4), 198–203. https://doi.org/10.1038/s41893-018-0047-7

57. Russo, G. S., Eftim, S. E., Goldstone, A. E., Dufour, A. P., Nappier, S. P., & Wade, T. J. (2020). Evaluating health risks associated with exposure to ambient surface waters during recreational activities: A systematic review and meta-analysis. *Water Research*, *176*, 115729. https://doi.org/10.1016/j.watres.2020.115729

58. Saikrishna, C. V., Rao, L. V., & Rao, D. M. (2024a). Assessment of Nagavali River water quality in and around Srikakulam District for agriculture and irrigation. *Rasayan Journal of Chemistry*, *17*(1), 28–37. https://doi.org/10.31788/RJC.2024.1718704

59. Saikrishna, C. V., Rao, L. V., & Rao, D. M. (2024b). Multivariate analysis for assessment of Vamsadhara River water quality, Andhra Pradesh, India. *Oriental Journal of Chemistry*, *40*(4), 1189–1198. https://doi.org/10.13005/ojc/400435

60. Sarma, V. V. S. S., Prasad, V. R., Kumar, B. S. K., Rajeev, K., Devi, B. M. M., Reddy, N. P. C., Sarma, V. V., & Kumar, M. D. (2010). Intra-annual variability in nutrients in the Godavari estuary, India. *Continental Shelf Research*, *30*(19), 2005–2014. https://doi.org/10.1016/j.csr.2010.10.001

61. Shivani, G., & Rao, L. M. (1996). The fishery of Gosthani estuary, near Visakhapatnam. *Indian Journal of Fisheries*, *43*(4), 371–374.

62. Spearman, C. (1904). The proof and measurement of association between two things. *The American Journal of Psychology*, *15*(1), 72–101. https://doi.org/10.2307/1412159

63. Sridevi, B., Vaury, V., Kumar, B. S. K., Sarma, V. V. S. S., Cardinal, D., & Sebilo, M. (2023). Assessing seasonal nitrogen transformations in the Godavari estuary, India. *Estuarine, Coastal and Shelf Science*, *290*, Article 108404. https://doi.org/10.1016/j.ecss.2023.108404

64. Sriramadas, A., & Murty, M. S. (1975). Lithology and structure of the Eastern Ghats of Visakhapatnam, Andhra Pradesh. *Journal of Geological Society of India*, *16*(2), 188–192. https://doi.org/10.17491/jgsi/1975/160207

65. Streeter, H. W., & Phelps, E. B. (1925). *A study of the pollution and natural purification of the Ohio River: III. Factors concerned in the phenomena of oxidation and reaeration* (Public Health Bulletin No. 146). U.S. Public Health Service, Government Printing Office.

66. Subba Rao, N. (2009). Fluoride in groundwater, Varaha River Basin, Visakhapatnam District, Andhra Pradesh, India. *Environmental Monitoring and Assessment*, *152*(1–4), 47–60. https://doi.org/10.1007/s10661-008-0295-5

67. Sudha Rani, P., Sampath Kumar, G., Mukherjee, J., Srinivas, T. N. R., & Sarma, V. V. S. S. (2018). Perennial occurrence of heterotrophic, indicator and pathogenic bacteria in the coastal Bay of Bengal (off Visakhapatnam) – Impact of physical and atmospheric processes. *Marine Pollution Bulletin*, *127*, 412–423. https://doi.org/10.1016/j.marpolbul.2017.12.023

68. United Nations Environment Programme. (2024). *Progress on ambient water quality: Mid-term status of SDG indicator 6.3.2 and acceleration needs, with a special focus on health*. UN-Water.

https://www.unwater.org/publications/progress-ambient-water-quality-2024-update

69. United States Environmental Protection Agency. (2012). *Recreational water quality criteria* (EPA-820-F-12-058). Office of Water. https://www.epa.gov/wqc/2012-recreational-water-quality-criteria
70. United States Environmental Protection Agency. (2013). *Aquatic life ambient water quality criteria for ammonia – freshwater 2013* (EPA 822-R-13-001). Office of Water. https://www.epa.gov/wqc/aquatic-life-criteria-ammonia
71. Ward, J. H., Jr. (1963). Hierarchical grouping to optimize an objective function. *Journal of the American Statistical Association*, *58*(301), 236–244. https://doi.org/10.1080/01621459.1963.10500845
72. Water Resources Department, Government of Andhra Pradesh. (n.d.). *Thatipudi Project, Vizianagaram district*. Retrieved September 20, 2026, from https://irrigationap.cgg.gov.in/wrd/static/approjects/thatipudi.html
73. Wiedenmann, A., Krüger, P., Dietz, K., López-Pila, J. M., Szewzyk, R., & Botzenhart, K. (2006). A randomized controlled trial assessing infectious disease risks from bathing in fresh recreational waters in relation to the concentration of *Escherichia coli*, intestinal enterococci, Clostridium perfringens, and somatic coliphages. *Environmental Health Perspectives*, *114*(2), 228–236. https://doi.org/10.1289/ehp.8115
74. Wohl, E. (2017). The significance of small streams. *Frontiers of Earth Science*, *11*(3), 447–456. https://doi.org/10.1007/s11707-017-0647-y

Figures

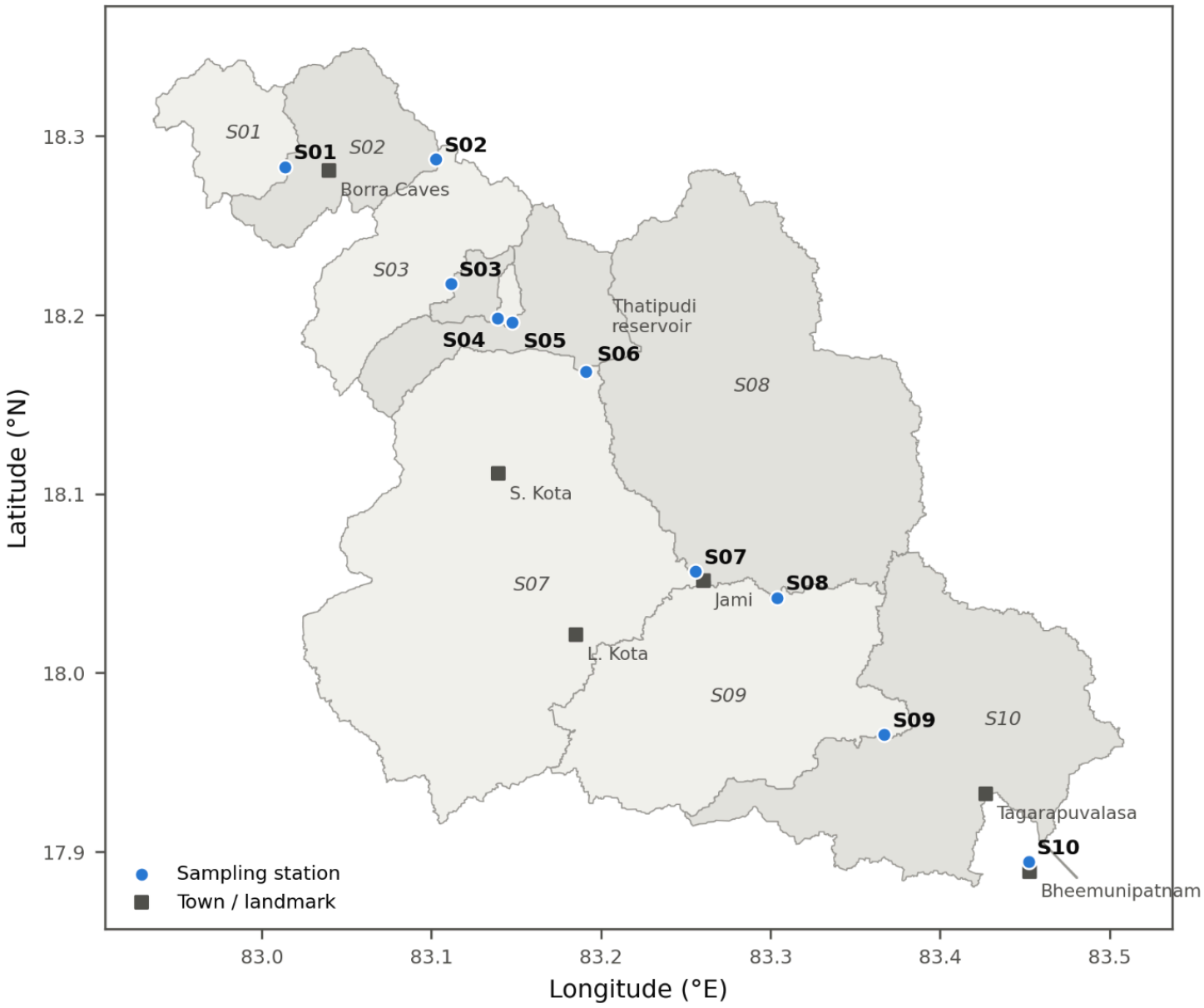


Figure 1

The Gosthani basin, the ten sampling stations and their incremental catchments delineated from the Copernicus GLO-30 digital elevation model

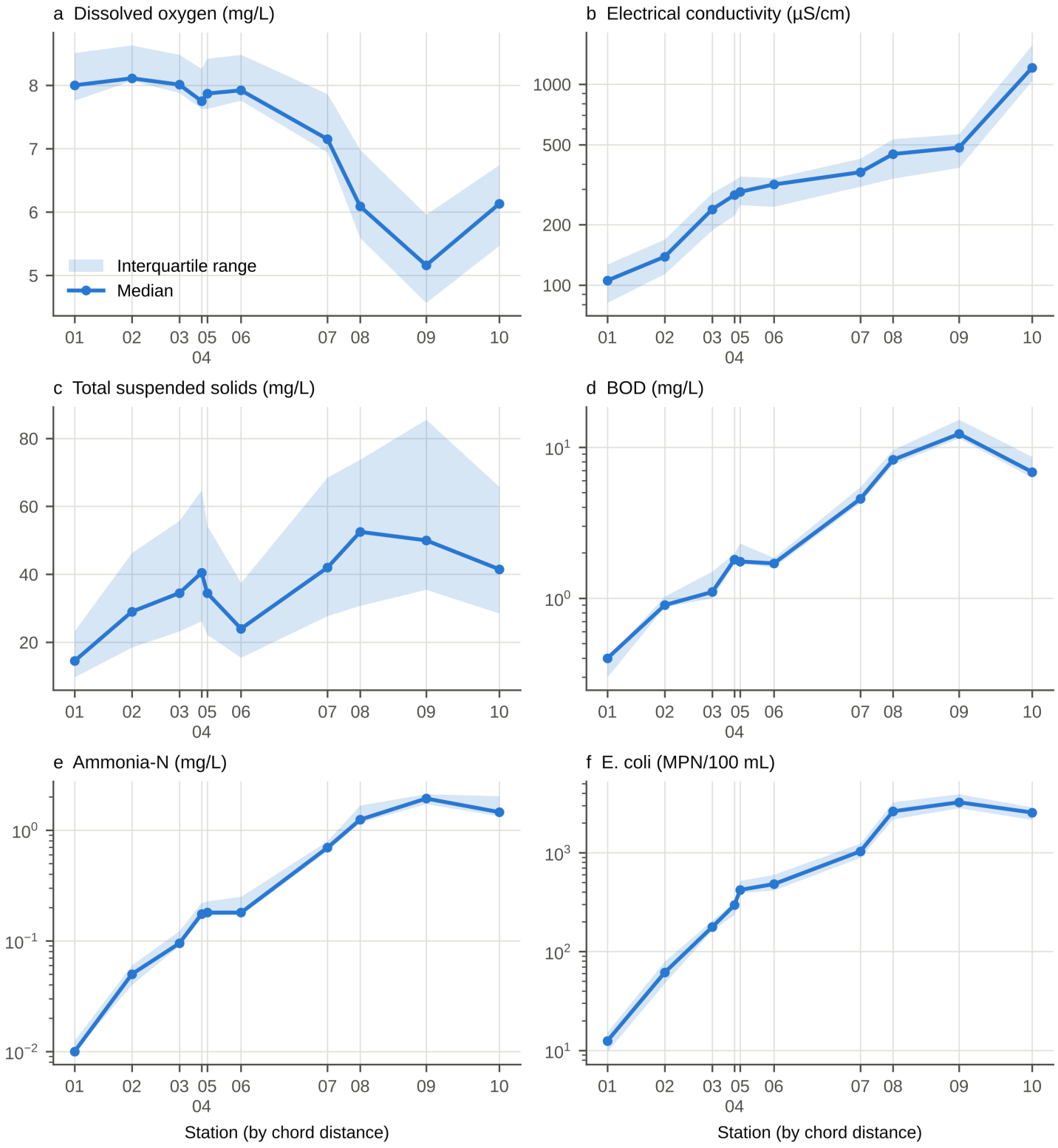


Figure 2

Station medians (line) and interquartile ranges (band) of six determinands (a–f), with stations spaced by chord distance from S01. Logarithmic axes for EC, BOD, ammonia-N and *E. coli*; n = 12 campaigns (13 for DO)

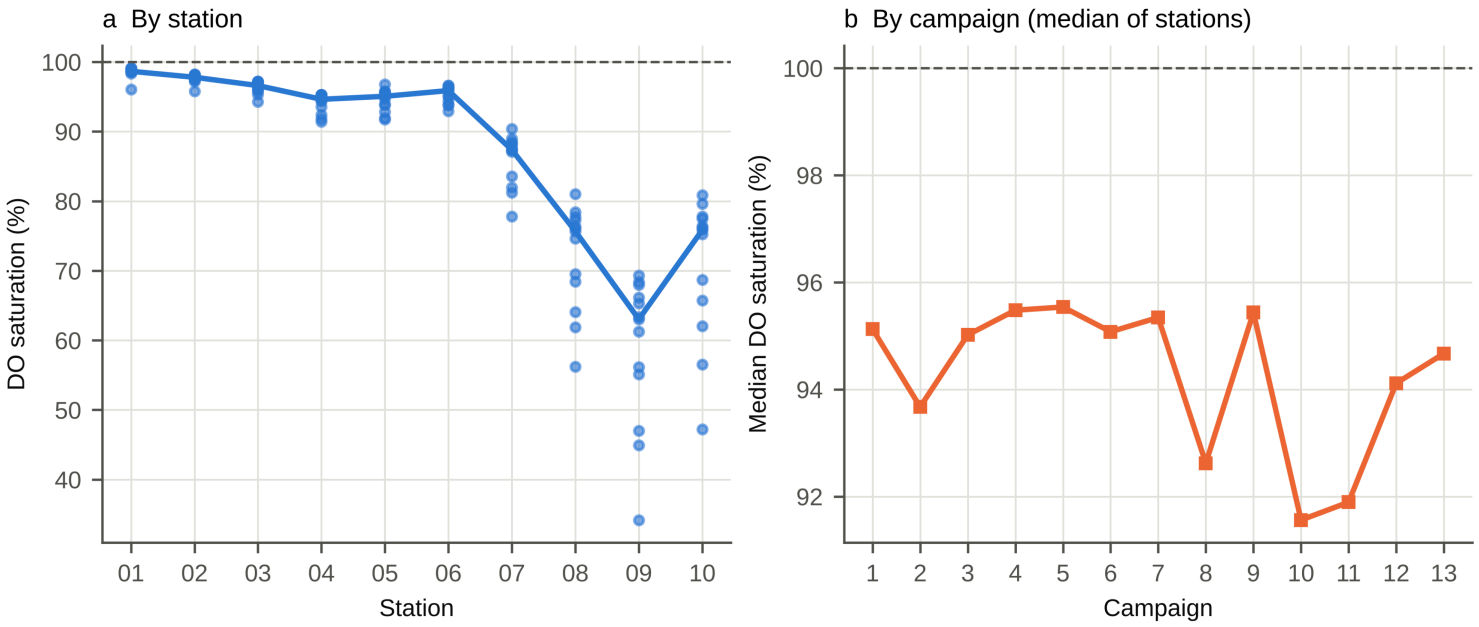


Figure 3

Dissolved-oxygen saturation (a) at each station in the 13 campaigns, with station medians (line), and (b) the median of the ten stations in each campaign. Dashed line, 100% saturation

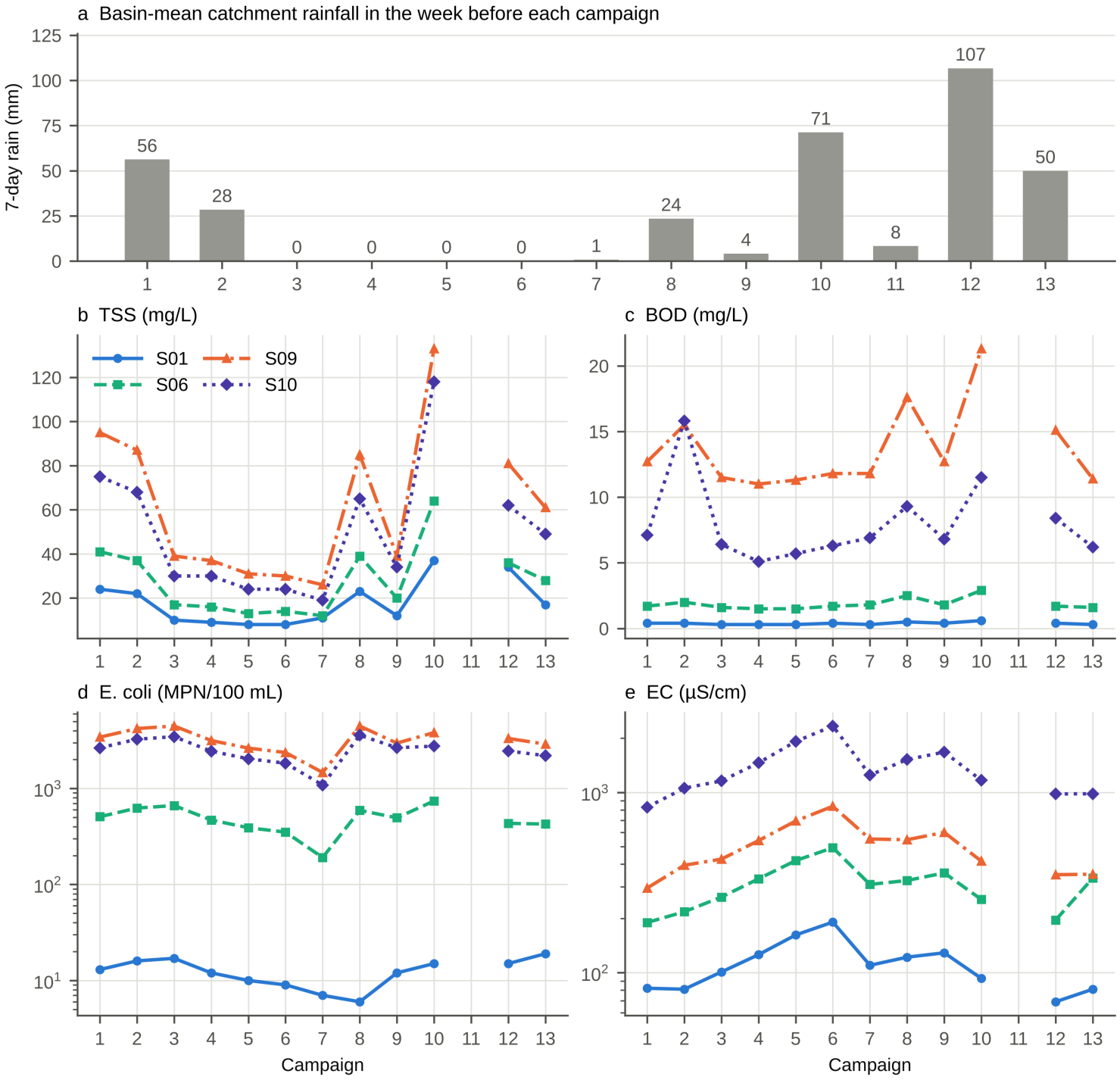


Figure 4

(a) Basin-mean 7-day catchment rainfall before each campaign and (b–e) total suspended solids, BOD, *Escherichia coli* and electrical conductivity at S01, S06, S09 and S10 (distinguished by line style and marker) in the 13 campaigns. Laboratory results for campaign 11 (July 2026) were excluded

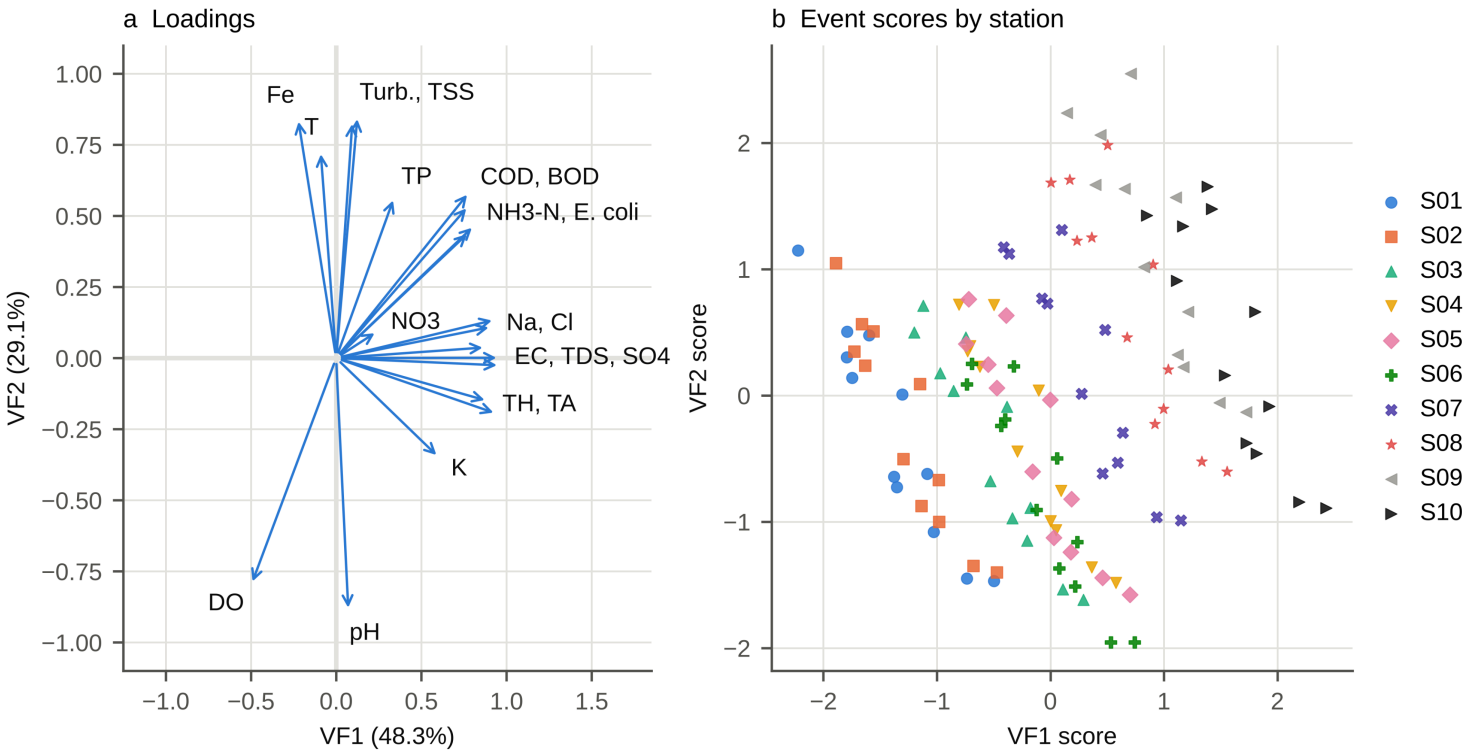


Figure 5

Principal component analysis of 20 determinands in 120 station-campaign observations: (a) varimax-rotated loadings on the first two components and (b) scores by station (distinguished by colour and marker shape)

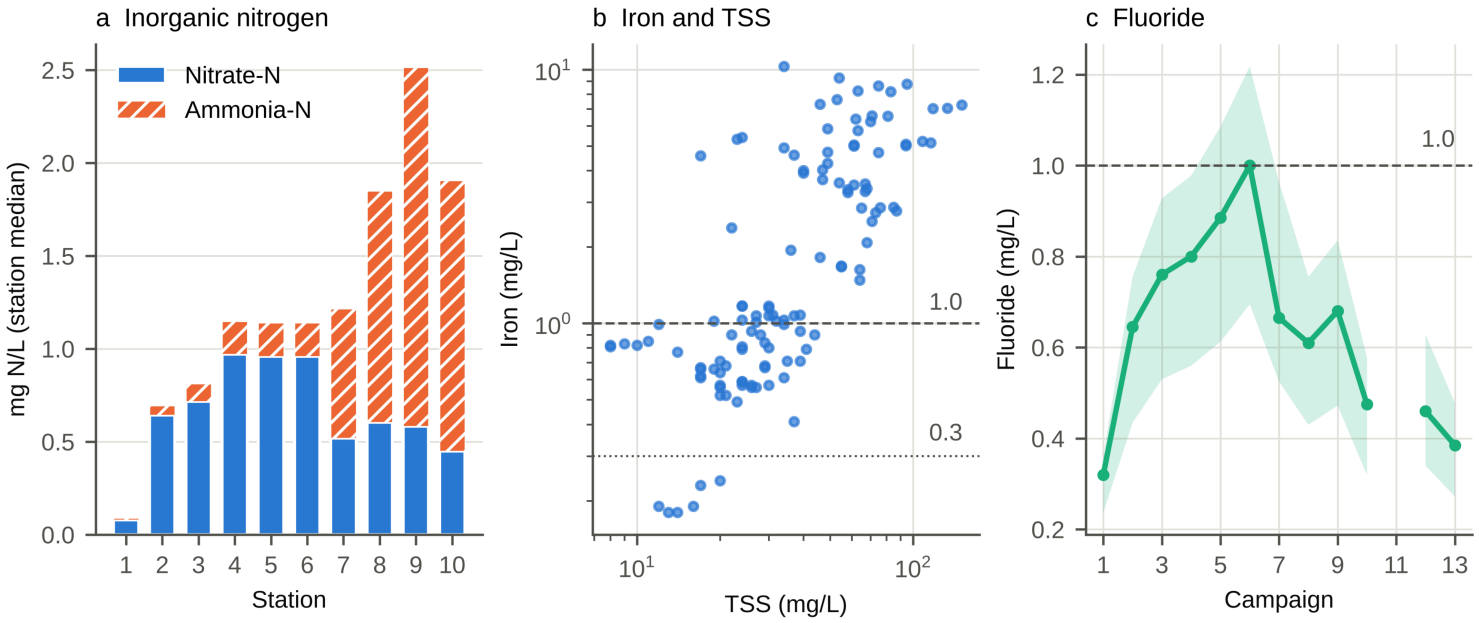


Figure 6

(a) Station medians of nitrate-N and ammonia-N; (b) iron versus total suspended solids for the paired observations, with the current IS 10500 acceptable limit (1.0 mg/L, dashed) and the limit before

Amendment No. 1 (0.3 mg/L, dotted); and (c) median and interquartile range of fluoride across stations in each campaign (July 2026 excluded)

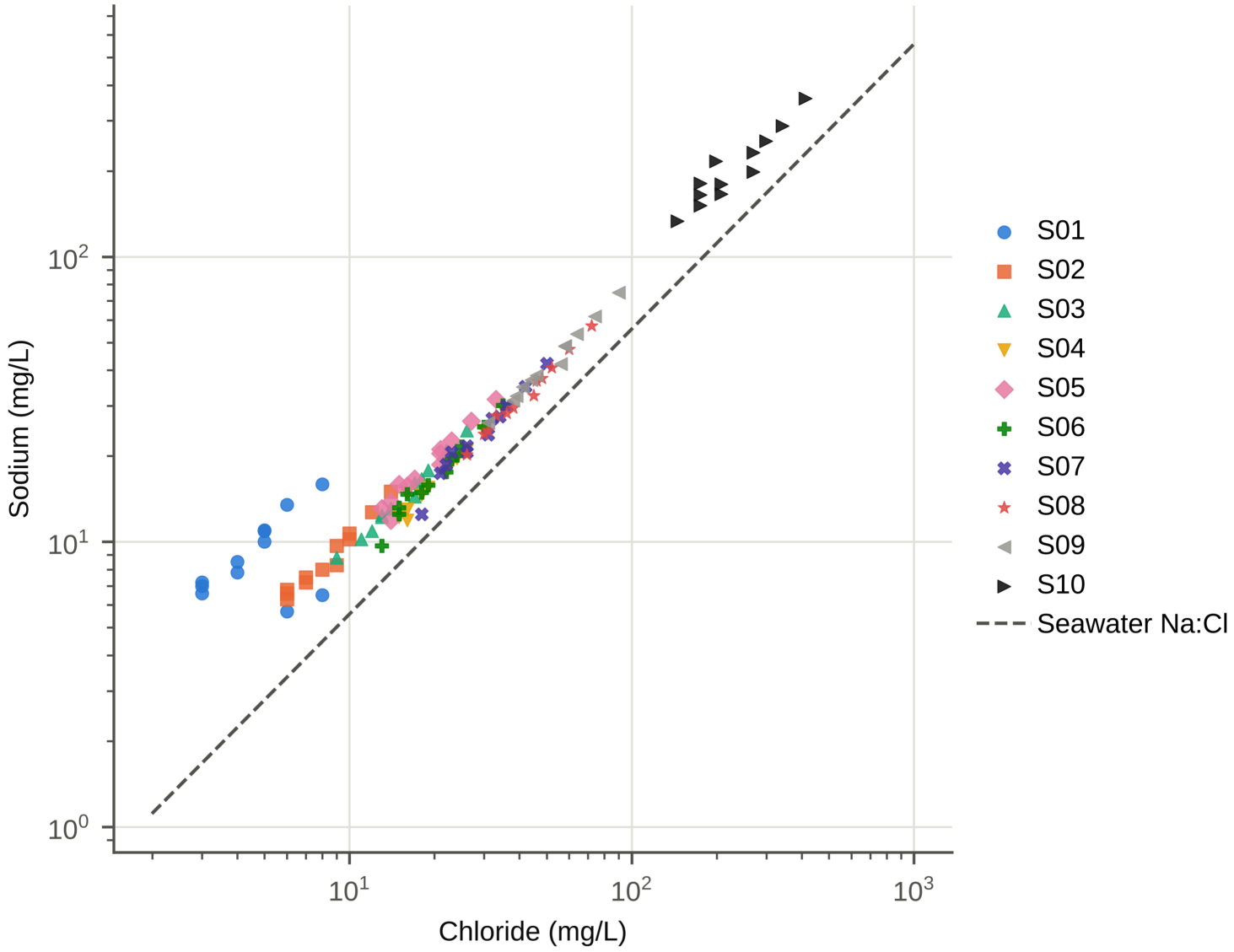


Figure 7

Sodium versus chloride for all observations, by station (colour and marker shape), with the mass ratio of standard seawater (dashed line)

Supplementary Files

This is a list of supplementary files associated with this preprint. Click to download.

- ESM2.xlsx